

Quantifying the $\delta^{15}\text{N}$ trophic offset in a cold-water scleractinian coral (CWC): implications for the CWC diet and coral $\delta^{15}\text{N}$ as a marine N cycle proxy.

Josie L. Mottram¹, Anne M. Gothmann², Maria G. Prokopenko³, Austin Cordova³, Veronica Rollinson¹, Katie Dobkowski⁴, Julie Granger¹

¹Department of Marine Sciences, University of Connecticut, Storrs, CT, 06340, USA

²Departments of Physics and Environmental Studies, St. Olaf College, Northfield, MN, 55057, USA

³Department of Geology, Pomona College, Claremont, CA, 91711, USA

⁴Department of Environmental Studies, Woodbury University, Burbank, CA, 91504, USA

Correspondence to: Anne M. Gothmann (gothma1@stolaf.edu)

Abstract. The nitrogen (N) isotope composition ($\delta^{15}\text{N}$) of cold-water corals is a promising proxy for reconstructing past ocean N cycling, as a strong correlation was found between the $\delta^{15}\text{N}$ of the organic nitrogen preserved in coral skeletons and the $\delta^{15}\text{N}$ of particulate organic matter exported from the surface ocean. However, a large offset of 8-9 ‰ between the $\delta^{15}\text{N}$ recorded by the coral and that of exported particulate organic matter remains unexplained. The 8-9 ‰ offset may signal a higher trophic level of coral dietary sources, an unusually large trophic isotope effect or a biosynthetic $\delta^{15}\text{N}$ offset between the coral's soft tissue and skeletal organic matter, or some combinations of these factors. To understand the origin of the offset and further validate the proxy, we investigated the trophic ecology of the asymbiotic scleractinian cold water coral *Balanophyllia elegans*, both in a laboratory setting and in its natural habitat. A long-term incubation experiment of *B. elegans* fed on an isotopically controlled diet yielded a canonical trophic isotope effect of 3.0 ± 0.1 ‰ between coral soft tissue and the *Artemia* prey. The trophic isotope effect was not detectably influenced by sustained food limitation. A long N turnover of coral soft tissue, expressed as an e-folding time, of 291 ± 15 days in the well-fed incubations indicates that coral skeleton $\delta^{15}\text{N}$ is not likely to track subannual (e.g. seasonal) variability of diet $\delta^{15}\text{N}$. Specimens of *B. elegans* from the subtidal zone near San Juan Channel (WA, USA) revealed a modest difference between soft tissue and skeletal $\delta^{15}\text{N}$ of 1.2 ± 0.6 ‰. The $\delta^{15}\text{N}$ of the coral soft tissue was 12.0 ± 0.6 ‰, which was ~6 ‰ higher than that of suspended organic material that was comprised dominantly of phytoplankton – suggesting that phytoplankton is not the primary component of *B. elegans*' diet. An analysis of size-fractionated net tow material suggests that *B. elegans* fed predominantly on a size class of zooplankton ≥ 500 μm , implicating a two-level trophic transfer between phytoplankton material and coral tissue. These results point to a feeding strategy that may result in an influence of regional food web structure on the cold-water coral $\delta^{15}\text{N}$. This factor should be taken into consideration when applying the proxy to paleoceanographic studies of ocean N cycling.

Formatted ... [1]

Deleted:

Deleted: ...as the ... [3]

Formatted ... [2]

Formatted ... [4]

Deleted: Zooplankton as the primary diet for cold-water scleractinian corals (CWCs): implications for the CWC marine N cycle proxy and trophic ecology.*

Formatted: Font color: Text 1

Formatted ... [5]

Deleted: sinking ...articulate organic matter exported from the surface ocean. However, a large offset of 8-9 ‰ between the $\delta^{15}\text{N}$ recorded by the coral and that of exported particulate organic matter remains unexplained. The 8-9 ‰ offset may signal a higher trophic level of coral dietary sources, potential sensitivity of the proxy to food web structure, ...n unusually large trophic isotope effect or a biosynthetic $\delta^{15}\text{N}$ offset between the coral's soft tissue and skeletal tissues ... [6]

Formatted ... [7]

Deleted: the

Deleted: .

Deleted: the ...oral skeleton is not apt ... [8]

Deleted: is not able to provide sufficient resolution to

Deleted:

Formatted ... [9]

Deleted: ity

Deleted: to record seasonal difference in

Deleted: shallow

Deleted: tissue ...¹⁵N of 1.2 ± 0.6 ‰. The $\delta^{15}\text{N}$ of the coral soft tissue was 12.0 ± 0.6 ‰, which was ~6 ‰ higher than that of suspended organic material that was comprised dominantly of phytoplankton – suggesting that phytoplankton the latter ... [10]

Formatted: Font: 12 pt, Font color: Auto

Formatted ... [11]

Deleted: portend

Deleted: sensitivity

Deleted: dependence

Deleted: ... This the ... factor should needed to ... [13]

Deleted: to on regional food web structure. This depende ... [14]

Formatted: Font: 12 pt, Font color: Auto

Formatted ... [12]

Deleted: heeded

Deleted: in

Formatted: Font: 12 pt, Font color: Auto

98 **1 Introduction**

99 Interactions between ocean circulation and nutrient cycling modulate the marine biological carbon pump,
100 the consequent partitioning of CO₂ between atmosphere and ocean, and thus influence planetary climate on
101 centennial to millennial time scales (Sigman and Boyle 2000). The marine nitrogen (N) cycle is highly sensitive
102 to these interactions, such that knowledge of modern and ancient ocean N cycling can help illuminate drivers of
103 past climate and contextualize modern global change (e.g., Altabet et al., 1994; Francois et al., 1997; Robinson
104 and Sigman 2008; Sigman et al., 1999; Kast et al. 2019).

105 The main tool to investigate the oceanic N cycle history is the nitrogen (N) isotope composition (i.e., the
106 ¹⁵N/¹⁴N ratio) of particulate organic nitrogen (PON) exported from the euphotic zone and preserved in various
107 paleo-archives, including bulk sedimentary N in anoxic sediments (reviewed by Robinson et al. 2023). Hereafter,
108 we express the ¹⁵N/¹⁴N ratio using delta notation (δ¹⁵N). The δ¹⁵N-PON recorded in paleo-oceanographic archives
109 reflects both regional N cycling processes and the balance of global ocean N source and sink terms (Sigman and
110 Fripiat 2019; Brandes and Devol 2002). In regions of the ocean where nitrate is quantitatively consumed, the
111 annually integrated δ¹⁵N-PON exported from the surface reflects the isotopic composition of thermocline nitrate
112 (Altabet et al. 1991). The latter is influenced by the circulation history of nitrate (e.g., Marconi et al., 2015), by
113 regional N₂ fixation (e.g., Casciotti et al. 2008; Knapp et al. 2008) and by water column denitrification (e.g.,
114 Pride et al., 1999; De Pol-Holz et al., 2007). In regions with incomplete consumption of surface nitrate, such as
115 Southern Ocean, the isotopic discrimination imparted during nitrate assimilation is reflected in the δ¹⁵N-PON,
116 which can be used to reconstruct the degree of surface nitrate consumption in the past (e.g., Sigman et al., 1999;
117 Francois et al. 1997).

118 Accurate interpretation of the N cycle's paleo-history relies on the presumption that the δ¹⁵N-PON preserved
119 in various palaeoceanographic archives is impervious to organic matter diagenesis. Bulk sedimentary δ¹⁵N
120 measurements are thus generally inadequate in this respect, subject to post-depositional processes (Robinson et
121 al. 2012) – barring fast-accumulating organic-rich anoxic sediments with negligible contribution from terrestrial
122 sources (e.g., Altabet et al., 2002; Ganeshram and Pedersen, 1998). To circumvent this limitation, several
123 “biological” archives of the δ¹⁵N-PON have been developed that are deemed resistant to diagenetic alteration.
124 These include the organic matter in diatom frustules and foraminifera tests (e.g., Ren et al., 2009; Robinson
125 and Sigman, 2008) and the organic matter in proteinaceous corals (e.g., Sherwood et al. 2009; Williams and
126 Grottooli 2010). Recently, the δ¹⁵N of organic N enclosed within the aragonite mineral lattice of asymbiotic
127 scleractinian (stony) cold-water corals (CWCs) has been found to reflect the δ¹⁵N-PON exported from the surface

Deleted:

Formatted: Font color: Text 1

Deleted: and

Deleted: , organic N in in soft corals, and organic N material preserved in foraminiferal tests and in diatom frustules

Deleted: Henceforth, we express the ¹⁵N/¹⁴N ratio in delta notation, where δ¹⁵N (‰ vs. air) = [((¹⁵N/¹⁴N_{sample})/(¹⁵N/¹⁴N_{air}) - 1]*1000. ...

Deleted: :

Formatted: Font color: Text 1

Formatted: No underline, Font color: Text 1

Formatted: Font color: Text 1

Formatted: No underline, Font color: Text 1

Formatted: Font color: Text 1

Formatted: No underline, Font color: Text 1

Formatted: Font color: Text 1

Formatted: Font color: Text 1

Deleted: intercalated

137 ocean (Wang et al., 2014), offering an exciting new archive of marine N cycling (Wang et al. 2017; Li et al.,
 138 2020, Studer et al., 2018; Chen et al. 2023). A robust cold-water coral archive of $\delta^{15}\text{N}$ -PON can complement the
 139 existing suite of nitrogen proxies by reducing the potential biases inevitable for almost any individual proxy,
 140 allowing for a broader geographic and temporal reconstruction, and increasing resolution of the proxy record.
 141 Foremost, as with foraminifera and diatom shells, organic material trapped within the coral's original aragonite
 142 mineral lattice is largely protected from diagenetic alteration (Drake et al. 2021), and compromised areas can be
 143 avoided by inspecting the skeletons for contamination and recrystallization (e.g., borings) using microscopic
 144 techniques (Gothmann et al. 2015). CWCs have a broad geographic distribution, being present in all ocean basins
 145 from the surface to 5000 m (Freiwald, 2002). CWCs also offer the potential to generate high-resolution records
 146 extending relatively far back in time, and corals have continuous skeletal accretion that records ocean conditions
 147 at the time of growth, so the analysis of multiple individuals provides enhanced temporal resolution of long-term
 148 records (Robinson et al., 2014; Hines et al. 2015). Unlike sediments containing microfossils (e.g. diatoms and
 149 foraminifera) CWC skeletons are not subject to bioturbation and absolute ages of this paleoarchive can be
 150 determined with decadal precision on the time scales of glacial-interglacial climate variability through U-Th
 151 series dating (Cheng et al., 2000; Goodfriend et al. 1992, Robinson et al., 2014, Li et al., 2020). Remarkably,
 152 individual coral samples can archive multiple seawater properties, such that a single CWC specimen can
 153 potentially be used to reconstruct deep (e.g., $\Delta^{14}\text{C}$, pH, temperature, and circulation proxies such as Ba/Ca
 154 and ϵNd) and surface ocean conditions ($\delta^{15}\text{N}$) at a precisely-known time (U-Th dating), making CWC unique as a
 155 paleoceanographic archive (Robinson et al., 2014; Thiagarajan et al., 2014; Rae et al. 2018).
 156 Yet an outstanding concern about the fidelity of the $\delta^{15}\text{N}$ of coral-bound organic N is a reported 8 - 9 ‰
 157 offset between coral-bound $\delta^{15}\text{N}$ and the corresponding $\delta^{15}\text{N}$ -PON exported to regions of coral growth (Wang et
 158 al. 2014). The magnitude of this offset substantially exceeds the 3 - 3.5 ‰ expected for a single trophic transfer
 159 (Minagawa and Wada 1984), assuming CWC feed predominantly on algal material exported from the surface
 160 ocean, Wang et al. (2014) explained the magnitude of the offset by arguing that CWCs feed on the more
 161 abundant pool of surface-derived suspended organic material (SPOM), as the $\delta^{15}\text{N}$ SPOM at depth is typically
 162 ~4-5‰ higher than that of sinking PON (Altabet 1988, Saino and Hattori, 1987). While CWCs are considered
 163 generalists with regard to diet (e.g., Mortensen, 2001; Freiwald, 2002; Carlier et al., 2009; Maier et al. 2023), a
 164 number of studies suggest that many species of CWC subsist predominantly on metazoan zooplankton prey (e.g.,
 165 Naumann et al. 2011; Kiriakoulakis et al. 2005; Purser et al. 2010; Tsounis et al. 2010). A zooplankton diet
 166 should result in an approximate two-level or more trophic transfer between surface PON and coral tissue (e.g.,

- Formatted: Font color: Text 1
- Formatted: Font color: Text 1
- Deleted: almost
- Deleted: each
- Formatted: Font color: Text 1
- Deleted: presumably
- Formatted: Font color: Text 1
- Deleted: .
- Deleted: ;
- Deleted: Corral skeletons can also be
- Deleted: ed
- Deleted: to avoid compromised areas
- Deleted: They
- Deleted: time
- Formatted: Font color: Text 1
- Formatted: Font color: Text 1
- Deleted: are
- Deleted: thus
- Deleted: directly dated with radiometric methods;
- Formatted: Font color: Text 1
- Formatted: Font color: Text 1
- Formatted: Font color: Text 1
- Deleted: Despite its promise,
- Formatted: Font color: Text 1
- Deleted: were
- Deleted: assuming that
- Deleted: to
- Deleted: (Duineveld et al. 2007; 2012)
- Deleted: reconciled this observation
- Deleted: of which
- Deleted: exported from the surface
- Deleted:
- Deleted: Duineveld et al. 2004; 2007; 2012; Kiriakoulakis et al. 2005, ...
- Deleted: , Dodds et al., 2009; van Oevelen et al. 2009
- Formatted: No underline, Font color: Text 1
- Formatted: Font color: Text 1
- Formatted: Font color: Text 1
- Deleted: ; Carlier et al. 2009; Dodds et al. 2009;
- Deleted: van Oevelen et al. 2009;

194 Sherwood et al. 2008), ~~closer~~ to the observed 8-9 ‰ offset, potentially rendering coral-bound $\delta^{15}\text{N}$ sensitive to
195 spatial and temporal differences in ~~trophic-level~~ food web structure. An alternative explanation for the offset is
196 that there is a large biosynthetic offset between the $\delta^{15}\text{N}$ of the CWC polyp and its skeletal tissue (Horn et al.
197 2011; Muscatine et al. 2005), assuming that CWCs' diet derives directly from sinking algal material from the
198 surface ocean. Otherwise, there could be an atypically large N isotope fractionation associated with the trophic-
199 level transfer between the coral diet and its tissue (>3-3.5‰), possibly borne out of intermittent starvation periods
200 (Doi et al., 2017), which is then ~~passed on~~ to the organic matrix within the coral skeleton. The gap in our
201 understanding of how corals record the $\delta^{15}\text{N}$ -PON exported from the surface ocean raises questions regarding the
202 consistency of the offset in space and time, and whether it is ~~likely~~ to differ among CWC species or due to intra-
203 specific variations in diet.

204 Due to the challenges of accessing deep ocean environments, the trophic ecology of cold-water corals is
205 sparsely documented, yet is fundamental to understanding the role of CWCs in cold-water reef ecosystems and to
206 defining their utility as paleoceanographic archives of N cycling. The nature of the $\delta^{15}\text{N}$ offset between CWC
207 skeletal material and exported PON must be explained in order to ~~further validate and potentially improve~~ the use
208 of ~~$\delta^{15}\text{N}$ of CWC skeletons as a proxy~~ to reconstruct the history of exported PON and to further understand the
209 role of CWCs in benthic ecosystems. To this end, we studied *Balanophyllia elegans*, an ~~asymbiotic~~ scleractinian
210 cold-water coral found along the west coast of North America that grows as individual polyps (Fadlallah, 1983).
211 We investigated the following questions: a) Is there a large offset in $\delta^{15}\text{N}$ between coral polyp tissue and coral
212 skeletal tissue? b) Is there an unusually large trophic-level offset between coral tissue and coral diet? c) Does *B.*
213 *elegans* feed predominantly on suspended particulate organic matter (SPOM) *in situ*? or d) does *B. elegans* feed
214 predominantly on metazoan zooplankton, resulting in a two-level trophic transfer between coral tissue and N of
215 export? To evaluate question (a), ~~we measured the $\delta^{15}\text{N}$ of tissue-skeleton pairs of coral samples collected in their~~
216 ~~natural habitat~~. To evaluate question (b), we cultured *B. elegans* corals in the laboratory ~~in experiments where~~
217 ~~both the isotopic composition of food and the frequency of feeding was controlled~~. To evaluate questions (c) and
218 (d), ~~we also investigated the $\delta^{15}\text{N}$ of various~~ components of the food web at a field site ~~where *B. elegans* are~~
219 ~~found plentifully~~. Our observations offer novel insights on the growth and trophic ecology of *B. elegans*,
220 providing unique new data on the N metabolism of CWC and their feeding ecology. We contextualize our
221 conclusions to inform the use of CWC archives as a paleo-proxy for marine N cycling and ocean
222 biogeochemistry.

223

Deleted: similar

Deleted: and

Deleted: lower

Deleted: communicated

Deleted: apt

Formatted: Font color: Text 1

Deleted:

Deleted:

Formatted: Font color: Text 1

Deleted: fully

Formatted: Font color: Text 1

Deleted:

Deleted:

Deleted: s

Deleted:

Deleted: ies

Formatted: Font color: Text 1

Formatted: Font color: Text 1

Deleted: s

Deleted:

Formatted: Font color: Text 1

Deleted: these

Deleted: s

Deleted: ,

Deleted: naturally-

Deleted: habitats

Deleted: under a controlled diet

Formatted: Font color: Text 1

Deleted: to document trophic isotope effects and soft tissue N turnover, ...we investigated the soft vs. skeletal tissue $\delta^{15}\text{N}$ of coral we investigated the soft vs. skeletal tissue $\delta^{15}\text{N}$ of coral specimens collected from a field site in the Salish Sea, and

Deleted: we investigated the soft vs. skeletal tissue $\delta^{15}\text{N}$ of coral collected from a field site in the Salish Sea, and

Deleted: w

Deleted: queried

Deleted: the

Formatted: Font: Not Italic, Font color: Text 1

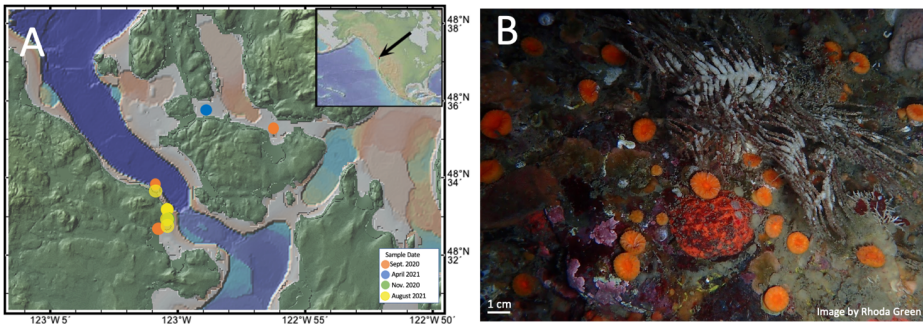
Deleted: .

Formatted: Font color: Text 1

255 2. Methods

256 2.1 Collection of live coral specimens

257 Individual specimens of the cold-water coral *Balanophyllia elegans* were collected during four sampling
258 campaigns in March and June 2019, and September and November 2020 from the San Juan Channel near the
259 University of Washington's Friday Harbor Laboratory off the coast of Washington State in the Salish Sea (48.5°
260 N, -123.0° W; Figure 1). *B. elegans* is a solitary, asymbiotic cold-water cup coral native to the Pacific Northwest
261 that can be found both in shallow rocky environments and at depths as great as 500 m (Durham and Barnard
262 1952). The genus *Balanophyllia* is cosmopolitan and fossil samples as old as Eocene in age have been used for
263 paleoenvironmental study (Muhs et al. 1994; Gothmann et al., 2015; Gagnon et al. 2021). *B. elegans*'s presence
264 at near surface depths makes it an easy target for culture experiments, and *Balanophyllia* sp. can be found co-
265 occurring with the similar but more widely applied cold-water coral archive, *Desmophyllum dianthus* (Margolin
266 et al. 2014). Therefore, we consider the asymbiotic *Balanophyllia* sp. to be generally representative of other deep
267 cold-water coral species.



268 Figure 1. (a) Map of the San Juan Islands indicating the collection site of *B. elegans* specimens and
269 hydrographic measurements (created using <http://www.geomapapp.org>, Ryan et al. 2009). Inset shows
270 where the San Juan Islands are situated within North America. (b) Image of *B. elegans* from the San
271 Juan Channel near Friday Harbor Labs taken by Rhoda Green.

268 *B. elegans* specimens were collected at 10 to 20 m depth by divers who gently removed the corals from
269 vertical rock walls using blunt-tipped diving knives. Of the live corals collected, a subset was immediately frozen
270 at -18°C for N isotope ratio analyses of soft tissue and organic matter bound in the coral skeleton matrix. Live
271 specimens were shipped overnight in small bags of seawater on ice to St. Olaf College (Minnesota, USA). Corals

Formatted: Font color: Text 1

Formatted: Font color: Text 1

Deleted: depths

Deleted: the

Deleted: but

Formatted: Font color: Text 1

Formatted: Font: (Default) +Headings (Times New Roman),
Font color: Text 1

Formatted: Font: (Default) +Headings (Times New Roman)

Formatted: Line spacing: single

Deleted: ESRI, 2021

Formatted: Font: (Default) +Headings (Times New Roman),
Font color: Text 1

Formatted: Font: 11 pt, Not Bold, Font color: Text 1

Formatted: Font: 11 pt, Not Bold, Font color: Text 1

Formatted: Font color: Text 1

Formatted: Font: (Default) +Headings (Times New Roman)

Deleted: S

Formatted: Indent: First line: 0.25", Line spacing: 1.5 lines

276 were cleaned by gently scraping the exposed skeleton with dental tools to remove encrusting organisms and
277 placed in incubation bottles with artificial seawater for recovery prior to feeding experiments (described below).

278 2.2 Live coral maintenance

279 Live *B. elegans* corals were maintained in artificial seawater medium prepared from nitrate-free Instant
280 Ocean® Sea Salt. Salts were dissolved in deionized water to a salinity of 28.0 ± 0.25 – akin to the conditions at
281 the collection site (Murray et al., 2015) – and sparged with air to achieve atmospheric equilibrium. The pH of the
282 seawater was measured with a YSI brand 4130 pH probe and adjusted using dilute (0.1 N) hydrochloric acid or
283 sodium hydroxide to 8.14 ± 0.05 , slightly higher than *in-situ* conditions to promote skeletal growth. Batch
284 seawater was then allotted to 2 L airtight polypropylene bottles to incubate single coral polyps. Bottles were pre-
285 cleaned with fragrance-free soap and multiple rinses of deionized water. The salinity, pH, and temperature in the
286 incubation bottles were monitored using YSI brand probes (4310(W) conductivity cell and pH probe,
287 respectively) as well as dissolved oxygen concentrations using an optical sensor (FDO 4410; Figure S1); a
288 Multilab 4010-3w was used as the digital meter for the sensors. The bottles containing individual corals were
289 randomly distributed among three recirculating water baths maintained at a constant temperature of 12.5 ± 0.2 °C,
290 akin to the conditions at the collection site (Murray et al., 2015). Small but quasi-systematic differences of \pm
291 0.3 °C were observed among the three recirculating tanks (Figure S2). Corals were sustained on a diet of *Artemia*
292 *salina* nauplii (described below), fed twice a week to ensure maximum growth (Crook et al., 2013). Seawater in
293 the incubation bottles was replaced twice a week after the corals were fed, based on observations indicating that
294 seawater pH in the bottles decreased slightly but significantly by ~ 0.03 pH units over three days due to coral
295 respiration (statistical analysis was performed with RStudio; Welch two sample t-test; $t(515.07) = 12.8$; p-value <
296 0.01 ; Figure S3). Dissolved oxygen concentrations remained near atmospheric equilibrium at concentration of 7.5
297 ± 0.3 mg L⁻¹ (Figure S1). Nitrate concentrations in the bottles were also monitored from samples taken during
298 each water change, in the freshly prepared seawater and in spent seawater, revealing low variability in NO₃⁻
299 concentration of 0.7 ± 0.3 μmol L⁻¹ (Figure S4). Nitrate concentrations in the incubations were notably lower than
300 ambient levels at the collection site, where concentration were ~ 25 μmol L⁻¹, ensuring that the coral's only source
301 of nitrogen was the *Artemia* diet (Murray et al., 2015).

Deleted: ¶



Formatted: Font color: Text 1

Formatted: Font color: Text 1

Formatted: Font color: Text 1

Formatted: Font color: Text 1

304 2.3 Coral culture experiments

305 2.3.1 *Experiment to quantify the trophic isotope effect*

306 The corals were acclimated to precise incubation conditions for approximately 20 hours before initiating
307 feeding experiments. To assess the $\delta^{15}\text{N}$ of coral soft tissue compared to that of its food source, four experimental
308 groups of individual *B. elegans* corals were fed respective diets of *Artemia salina* nauplii with different $\delta^{15}\text{N}$
309 values, twice per week for 530 days (Spero et al., 1993). Unhatched *Artemia salina* sourced from specific
310 geographic locations have widely different $\delta^{15}\text{N}$ values, owing to the different N isotope dynamics of the
311 environments from which they were collected, which makes these organisms useful for trophic studies (Spero et
312 al. 1993). Eighteen coral specimens were fed *Artemia* nauplii hatched from cysts from the Great Salt Lake
313 (Reference Code: GSL) with a $\delta^{15}\text{N}$ of 17.0 ± 0.3 ‰. Twelve corals were fed hatched nauplii from Lake Ulzhay
314 in Russia (Reference Code: 1816) with a $\delta^{15}\text{N}$ of 13.8 ± 0.4 ‰. Twelve corals were fed hatched nauplii from
315 Vinh Chau in Vietnam (Reference Code: 1805) with a $\delta^{15}\text{N}$ of 9.9 ± 0.3 ‰. Twelve corals were fed hatched
316 nauplii from Tibet (Reference Code: 1808) with $\delta^{15}\text{N}$ of 6.3 ± 0.2 ‰. The GSL *Artemia* was procured from
317 Aquatic Foods California Blackworm Co. (Great Salt Lake), whereas all other *Artemia* were obtained from the
318 *Artemia* Reference Center (Ghent, Belgium). The $\delta^{15}\text{N}$ of the diet for each treatment was calculated as the mean
319 value measured from each group of unhatched cysts and hatched nauplii (Table S2 and S3).

320 Fresh batches of nauplii were hatched from *Artemia* cysts at approximately monthly intervals, filtered into a
321 concentrated suspension, stored frozen at -18°C , and thawed immediately before feeding to the corals. Due to low
322 hatch rates of the *Artemia* group 1808, corals in that treatment group were fed nauplii harvested from
323 decapsulated *Artemia* cysts from day 151 (November 19, 2019) to 245 (February 22, 2020). The $\delta^{15}\text{N}$ of the
324 hatched nauplii ranged from 6.3 ± 0.2 to 17.0 ± 0.3 ‰ (measured by EA-IRMS; Table S2). The $\delta^{15}\text{N}$ of the
325 nauplii did not change significantly over prolonged storage of several months in the freezer (ANOVA test; $F(1) =$
326 0.07 , $p\text{-value} = 0.80$; Figure S5). *Artemia* nauplii had a statistically indistinguishable molar C:N ratios among
327 regional groups, averaging 6.0 ± 0.6 (ANOVA test; $F(3) = 0.31$; $p\text{-value} = 0.82$, Table S3). These results show
328 that there was limited variability in the diet of corals due to freezer storage and hatching of multiple individual
329 batches of *Artemia* (Table S2, S3, Figure S5).

330 Corals were fed their respective nauplii diets by transferring coral individuals from their incubation bottle to
331 a small dish filled with artificial seawater with minimal exposure to air so as not to stress the corals. Each coral
332 was fed 20 μL of thawed nauplii suspension by pipetting the food directly into their oral cavity, making it
333 possible to visually ensure complete consumption and thus minimize variability in feeding rates. Each coral was

Deleted: Evaluation of the trophic isotope effect and turnover time

Formatted: Font color: Text 1

Deleted: We refer to respective experimental groups by a color name (green, yellow, orange and pink).

Deleted: assigned to the green group

Deleted: The yellow group consisted of t

Deleted: that

Formatted: Font color: Text 1

Deleted: in the orange group which was

Formatted: Font color: Text 1

Deleted: The pink group consisted of t

Deleted: that

Formatted: Font color: Text 1

Formatted: Font color: Text 1

Formatted: Font color: Text 1

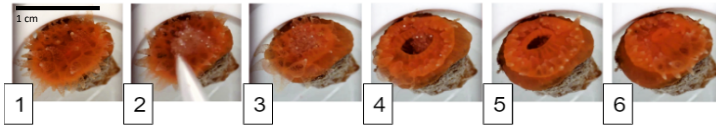
Deleted: 3

Formatted: Font color: Text 1

Formatted: Line spacing: 1.5 lines

345 returned to its bottle with a fresh allotment of seawater when its mouth had remained closed for several minutes,
346 signifying that it was finished eating (Figure 2).

347 After a shift in the $\delta^{15}\text{N}$ of diet, it is expected that coral tissue $\delta^{15}\text{N}$ will evolve as a function of time until the
348 composition of tissue reaches an equilibrium in line with the new diet. In order to assess the rate (referred to here
349 as the isotopic turnover time) at which this evolution occurs, individual corals were sacrificed at discrete intervals
350 throughout the experiment. Corals were always sacrificed three days after feeding to ensure that no food
351 remained in the oral cavity. The corals were removed from their bottles and rinsed with artificial seawater. The
352 coral tissue was then separated from the skeleton using a fine stream of compressed air. The tissue and skeleton
353 were frozen at -18°C and stored separately until processed for isotope ratio analyses.



347 **Figure 2.** Photo illustration of a coral feeding sequence. Photo 1 shows coral before food is given. Photo 2
348 shows food being pipetted onto coral mouth. Photos 3 through 6 show the coral feeding as the mouth opens to
349 engulf food and closes when finished, about 15 minutes in total. Corals are ~1 cm in diameter.

354 2.3.2 Experiment to evaluate the effects of starvation conditions

355 An additional 522-day feeding experiment was performed to assess the influence of starvation on the $\delta^{15}\text{N}$ of
356 the coral soft tissue. Live corals collected during a sampling campaign at the end of November 2020 and shipped
357 live to St. Olaf College were randomly assigned to two treatment groups (starved and not-starved). Corals in the
358 starved treatment were fed at 25% of our normal feeding frequency, or every two weeks, whereas those in the
359 not-starved treatment were fed twice a week. These feeding regimes were chosen based on the work of Crook et
360 al. (2013) and Beauchamp et al. (1989), who assumed feeding every 3 days to represent plentiful food supply and
361 feeding every 21 days (close to our starvation condition) to represent minimal maintenance food supply. Both
362 groups were fed *Artemia* nauplii with a $\delta^{15}\text{N}$ of 9.9 ± 0.3 ‰, approximately 3 ‰ lower than the coral tissue of
363 average *B. elegans* collected from Friday Harbor, and thus presumably closest in $\delta^{15}\text{N}$ to what the corals is eating
364 in the wild given a canonical trophic isotope effect. Coral incubations and feedings were conducted as described
365 above. Individuals were sacrificed over the course of the 522-day experiment, and tissue samples were frozen at
366 -18°C until isotope analysis.

Formatted: Font color: Text 1

Formatted: Font color: Text 1

Formatted: Font color: Text 1

Moved (insertion) [2]

Formatted: Font color: Text 1

Formatted: Font color: Text 1

Moved up [2]: Corals were always sacrificed three days after feeding to ensure that no food remained in the oral cavity. The corals were removed from their bottles and rinsed with artificial seawater. The coral tissue was then separated from the skeleton using a fine stream of compressed air. The tissue and skeleton were frozen at -18°C and stored separately until processed for isotope ratio analyses.

Moved (insertion) [1]

Deleted: Individual corals were sacrificed at discrete intervals throughout the experiment to monitor N turnover. Corals were always sacrificed three days after feeding to ensure that no food remained in the oral cavity. The corals were removed from their bottles and rinsed with artificial seawater. The coral tissue was then separated from the skeleton using a fine stream of compressed air. The tissue and skeleton were frozen at -18°C and stored separately until processed for isotope ratio analyses.

Deleted: ¶

¶

Deleted: In order to determine the trophic $\delta^{15}\text{N}$ offset between tissue and prey and to estimate the turnover time of the coral tissue with respect to nitrogen, we fit the data to a least-squares regression corresponding to an isotope mixing model in which describes the time-dependent evolution of tissue $\delta^{15}\text{N}$ in relation to that of the diet (Eq. 1, after Cerling et al. 2007; Ayliffe et al. 2004), ¶
$$N = + + \epsilon. \quad \text{Equation 1}^\dagger$$

The term $\delta^{15}\text{N}_{t=0}$ is the value of the coral tissue at the onset of the experiment, $\delta^{15}\text{N}_{\text{diet}}$ is that of the corals' *Artemia* diet, t is the number of days since the start of the experiment, ϵ is the difference between the $\delta^{15}\text{N}$ of the diet and tissue at equilibrium, and λ is the specific nitrogen incorporation rate (d^{-1}), the inverse of which is the turnover time for N. Values of ϵ and λ were estimated by generating 4 simultaneous equations using the $\delta^{15}\text{N}$ of soft tissue and diet for the 4 treatments groups. ¶

Deleted: E

Deleted: ion of

Formatted: Font color: Text 1

Deleted: , referred to as "long" and "short".

Deleted: "long"

Deleted: weeks,

Deleted: "short"

405 2.4 Coral preparation for isotope ratio analyses

406 Frozen coral tissue samples (and hatched nauplii) were freeze-dried using a Labconco FreeZone 4.5 and then
407 powdered using a mortar and pestle. The samples were sent to the University of Connecticut, Avery Point
408 (Groton, CT, USA) for isotope ratio analyses.

409 Coral skeletons from specimens collected at Friday Harbor were separated from the coral soft tissue and were
410 rinsed and individually ultrasonicated two times in Milli-Q™ (MQ) water for 20 minutes each in order to
411 remove any residual seawater. Samples were then individually ultrasonicated in a 1% sodium hypochlorite
412 (bleach) solution for at least two 20-minute intervals with fresh bleach for each new ultrasonication interval until
413 no tissue remained on the skeleton, as assessed visually under a dissection microscope. Individual skeletons were
414 then rinsed and ultrasonicated for 20 minutes in MQ another three times (each time with a new batch of MQ
415 water) in order to remove any bleach residue. Skeleton samples were sent to Pomona College (California, USA)
416 for further processing.

417 It is necessary to isolate organic matter from the coral carbonate matrix in advance of the N isotope
418 measurement methods used here (see Section 2.6 below). Organic material in the skeleton matrix was isolated
419 and oxidized to nitrate following the protocol of Wang et al. (2014). Briefly, bulk samples weighing 50-100 mg
420 were ground into coarse powder, and a fraction between 63 and 200 μm was collected by sieving through two
421 metal sieves. The 10-15 mg of sieved powder was rinsed sequentially with of sodium polyphosphate-sodium
422 bicarbonate buffered dithionite-citrate reagent, then treated with 13.5% sodium hypochlorite overnight on a
423 shaker. Skeletal material was dissolved in 4 N ultrapure hydrochloric acid, then oxidized to nitrate by autoclaving
424 in basic potassium persulfate solution. Standards of glutamine reference material USGS-40 and USGS-41
425 (respective δ¹⁵N of 4.52 ‰ vs. air and 47.57 ‰ vs. air) were oxidized in tandem and used to correct for
426 processing blanks. The resulting nitrate samples were sent to the University of Connecticut for nitrate isotope
427 ratio analysis. The long-term averaged reagent blank was 0.4-0.6 μmol L⁻¹, while the typical samples were 10-15
428 μmol L⁻¹ (typical amount of nitrogen in skeleton being 2-5 μmole/g of aragonite). Samples were typically run in
429 duplicates with an average reproducibility of ~ ± 0.5 ‰. An internal laboratory standard of ground material of the
430 cold-water colonial scleractinian coral *Lophelia pertusa* had a long-term δ¹⁵N value 9.4 ± 0.8 ‰ (n=57)

431 2.5 Hydrographic data

432 To infer the natural food source of the *B. elegans*, we collected samples for analysis of the δ¹⁵N of particulate
433 and dissolved N pools in relation to ambient hydrographic variables (temperature and salinity) near Friday

Formatted: Font color: Text 1

Deleted: separate

Deleted: ,

Deleted: .

Formatted: Font color: Text 1

Formatted: Font color: Text 1

Formatted: Font color: Text 1

Formatted: Font color: Text 1

Formatted: Font color: Text 1

Deleted: .

Deleted:

Formatted: Font color: Text 1

Formatted: Font color: Text 1

Deleted:

Deleted: 8.8

Deleted: 1.2

Deleted: 106

Formatted: Font color: Text 1

Formatted: Font color: Text 1

Formatted: Font color: Text 1

443 Harbor, WA. Seasonal sampling campaigns were conducted in September and November 2020 and in April,
444 June, and August 2021 (Table S1). In all but the August 2021 campaign, particulate and dissolved N samples
445 were collected by divers at unspecified depths between the surface and the depth of coral collection. Samples
446 were stored frozen in 30 mL HDPE bottles. Surface net tows were performed with a mesh size of 120 μm ;
447 materials were stored and shipped frozen and thawed at a later time to be filtered onto pre-combusted GF/F filters
448 (0.7 μm nominal pore size) that were stored frozen pending isotope analysis. No hydrographic variables were
449 recorded during the campaigns except in August 2021.

450 During the August 2021 campaign, depth profiles of temperature and salinity from the surface to 35 m were
451 characterized with a CastAway®-CTD (conductivity temperature depth) profiler. Water samples were collected
452 at 5 m intervals between 5 and 30 m using a Van Dorn water sampler. Water was filtered onto pre-combusted
453 glass fiber filters (GF/F; 0.7 μm nominal pore size) into pre-cleaned 30 mL HDPE bottles and stored frozen
454 pending analyses of nitrate concentrations and nitrate isotope ratios. The corresponding filters were stored frozen
455 for isotope ratio analysis of suspended particulate organic material (SPOM). Surface (5 m) and deeper (25 m to
456 the surface) net tows were conducted using plankton nets with respective mesh sizes of 150 μm and 80 μm . Net
457 tow material was filtered directly onto a pre-combusted GF/F filters and frozen pending analysis. A portion of the
458 net tow material from the August 2021 campaign was sieved to separate size classes of 80-100 μm , 100-250 μm ,
459 $\geq 250\mu\text{m}$, 250-500 μm , and $\geq 500 \mu\text{m}$. Material from the respective size classes was filtered onto pre-combusted
460 GF/F filters and frozen until isotope analysis.

461 2.6 Nitrate concentrations and isotope ratio analyses

462 Nitrate concentrations of oxidized coral skeletons and in aqueous samples were measured by reduction to
463 nitric oxide in hot vanadium III solution followed by chemiluminescence detection of nitric oxide (Braman and
464 Hendrix, 1989) on a Teledyne chemiluminescence NOx analyzer Model T200 (Thousand Oaks, CA).

465 The $\delta^{15}\text{N}$ and $\delta^{13}\text{C}$ of lyophilized coral tissue samples were analyzed at the University of Connecticut on a
466 Costech Elemental Analyzer–Isotope Ratio Mass Spectrometer (Delta V) and are expressed in standard delta
467 notation (e.g. for N, $\delta^{15}\text{N}$ (‰ vs. air) = $[(^{15}\text{N}/^{14}\text{N}_{\text{sample}})/(^{15}\text{N}/^{14}\text{N}_{\text{air}})] - 1$)*1000). Approximately 0.75 mg of
468 lyophilized sample (35 μg N) was allotted into tin cups and analyzed in tandem with recognized glutamine
469 reference materials USGS-40 and USGS-41 with respective $\delta^{15}\text{N}$ (vs. air) of 4.52 ‰ and 47.57 ‰ and $\delta^{13}\text{C}$ of -
470 26.39 ‰ and 37.63 ‰ (vs. PDB). Replicate analyses of ($n \geq 2$) reference materials yielded an analytical precision
471 of (± 1 SD) of 0.3‰ for both $\delta^{15}\text{N}$ and $\delta^{13}\text{C}$.

Deleted: undefined

Formatted: Font color: Text 1

Formatted: Line spacing: 1.5 lines

Formatted: Font color: Text 1

Deleted: 5

474 Nitrate N (and O) isotope ratios of aqueous seawater samples and N isotope ratios of the skeleton matrix
 475 samples were analyzed at University of Connecticut using the denitrifier method (Casciotti et al., 2002; McIlvin
 476 and Casciotti, 2011; Sigman et al., 2001). Nitrate sample solutions were injected at target concentrations of 20
 477 nmol for seawater samples and 7 nmol for skeleton matrix samples. N₂O was extracted, concentrated and purified
 478 using a custom-modified Thermo Gas Bench II equipped with a GC Pal autosampler and dual cold traps and
 479 analyzed on a Thermo Delta V Advantage continuous flow isotope ratio mass spectrometer (Casciotti et al., 2002;
 480 McIlvin and Casciotti, 2011). Individual analyses were referenced to injections of N₂O from a pure gas cylinder
 481 and standardized through comparison potassium nitrate reference materials International Atomic Energy Agency
 482 nitrate (IAEA-N3) and the isotopic nitrate reference material United States Geological Survey 34 (USGS-34),
 483 with respective δ¹⁵N vs. air of 4.7 ‰ and -1.8 ‰ vs. air (International Atomic Energy Agency, 1995), and
 484 respective δ¹⁸O of 25.61 ‰ and -27.9 ‰ vs. Vienna Standard Mean Ocean Water (VSMOW; Gonfiantini, 1995;
 485 Böhlke et al., 2003). To account for bacterial blanks and source linearity, nitrate concentrations of the standard
 486 material – diluted in N-free seawater for aqueous seawater samples and air-equilibrated milli-Q water for
 487 skeleton matrix samples – were matched to those of samples within batch analyses, and additional bacterial
 488 blanks were also measured (Weigand et al., 2016; Zhou et al., 2022). Replicate measurements (n ≥ 2) of all
 489 samples yielded an average analytical precision (±1 SD) of 0.3‰ for both δ¹⁵N and δ¹⁸O.

491 2.7. N turnover model

492 We estimate values of the trophic δ¹⁵N offset for *B. elegans*, ϵ , and the rate of isotopic turnover by fitting
 493 the data from our trophic isotope experiment to a nonlinear least-squares regression model corresponding to the
 494 isotope mixing relationship shown in Equation 1 below. Equation 1 treats the coral tissue as a single reservoir of
 495 N with some initial isotope composition that is evolving to reflect the new diet as a function of time (after Cerling
 496 et al. 2007; Ayliffe et al. 2004).

$$497 \delta^{15}N(t) = [\delta^{15}N_{t=0} - \delta^{15}N_{diet} + \epsilon] \cdot e^{-\lambda t} + \delta^{15}N_{diet} + \epsilon. \quad \text{Equation 1}$$

498 The term δ¹⁵N_{t=0} is the value of the bulk coral tissue at the onset of the experiment, δ¹⁵N_{diet} is that of the corals'
 499 new *Artemia* diet (i.e. what it is fed during the experiment), t is the number of days since the start of the
 500 experiment, ϵ is the difference between the δ¹⁵N of the diet and tissue at equilibrium (i.e. once the isotopic
 501 composition of inputs to the system equals the isotope composition of outputs), and λ describes the specific rate
 502 at which new N is incorporated into the coral tissue (days⁻¹). We use this model to calculate the e-folding time of

Formatted: Font color: Text 1

Formatted: Font color: Text 1

Formatted: Font color: Text 1

Deleted: es

Deleted: es

Deleted: The denitrifier method uses denitrifying bacteria (*Pseudomonas chlororaphis* f. sp. *aureofaciens*, ATCC 13985) that lack the terminal nitrous oxide (N₂O) reductase to quantitatively convert nitrate to nitrous oxide which is measured by gas-chromatography-isotope ratio mass spectrometry. Cells were cultured in Tryptic Soy Broth (Difco; Hunt Valley, MD, USA) amended with 10 mM nitrate in stoppered glass bottles. Cells in stationary phase were harvested by centrifugation and resuspended in nitrate-free medium and dispensed as 3 mL aliquots into 10 mL glass vials, which were then sparged with dinitrogen (N₂) gas for approximately 6 hours to remove N₂O. Nitrate sample solutions (20 nmol for seawater samples and 7 nmol for skeleton matrix samples) were injected into the sparged vials and incubated overnight to allow for complete conversion of nitrate to N₂O gas.

Deleted: ¶

Deleted: The product

Formatted: Font color: Text 1

Formatted: Font color: Text 1

Formatted: Font color: Text 1

Formatted: Font color: Text 1

Deleted: ¶

Formatted: Underline

Formatted: Indent: First line: 0", Line spacing: 1.5 lines

522 the system, which is defined as $1/\lambda$ (days) and represents the time at which ~63% of the original N reservoir in
523 coral tissue has been replaced with new N from the experimental coral diet.

525 3. Results

526 3.1 Trophic isotope effect

527 At the onset of the culture experiment, the soft tissue among all experimental corals had a $\delta^{15}\text{N}$ of 11.7 ± 0.5
528 ‰. Over the course of the experiment, the $\delta^{15}\text{N}$ of the tissue increased or decreased in respective treatments
529 depending on the $\delta^{15}\text{N}$ of their *Artemia* diet (Figure 3); the tissue $\delta^{15}\text{N}$ increased in corals fed diets with $\delta^{15}\text{N}$
530 values of 17.0, 13.8, and 9.9 ‰, whereas the tissue $\delta^{15}\text{N}$ decreased for the diet of 6.4 ‰. The $\delta^{15}\text{N}$ of soft tissue
531 in all groups trended towards an asymptotic offset relative to the diet $\delta^{15}\text{N}$, as expected for an approach to a new
532 equilibrium. However, at day 530, at the end of the experiment, it appeared as though the coral tissue $\delta^{15}\text{N}$ had
533 not yet reached a constant offset value, suggesting that the coral tissue had not yet reached an equilibrium with

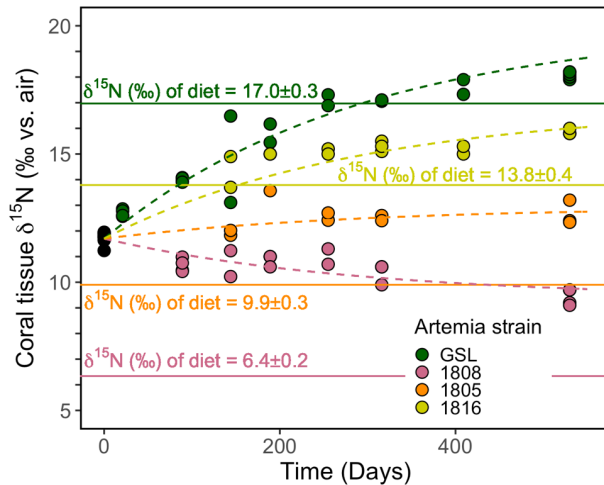


Figure 3. Evolution of the coral soft tissue $\delta^{15}\text{N}$ in response to diet $\delta^{15}\text{N}$. Colors correspond to the respective *Artemia* strains. Dashed lines are the model output of our simultaneous nonlinear least squares regression fits to the data using Equation 1. Solid lines mark the diet $\delta^{15}\text{N} \pm \sigma$. The mean analytical error on tissue $\delta^{15}\text{N}$ analyses was ± 0.2 ‰.

540 the new diet. Specifically, at the end of the experiment, the coral tissue of the treatment groups reached $\delta^{15}\text{N}$
541 values of $9.4 \pm 0.3\%$, $12.6 \pm 0.5\%$, $15.9 \pm 0.1\%$, and $18.1 \pm 0.1\%$ for groups fed the lowest to highest *Artemia*
542 $\delta^{15}\text{N}$ values, respectively. The difference between coral soft tissue and diet $\delta^{15}\text{N}$ ranged from a minimum of $1.0 \pm$
543 0.1% to a maximum of $3.0 \pm 0.3\%$ across the different experimental groups at day 530 (Figure 3).

544 Despite the fact that coral tissue had not yet reached an equilibrium with the new coral diet at the end of our
545 experiment, we are able to estimate values of the trophic $\delta^{15}\text{N}$ offset for *B. elegans*, ϵ , and the rate of isotopic
546 turnover by fitting the data from our trophic isotope experiment to the nonlinear least-squares regression model
547 given Equation 1 in Section 2.7. To more confidently calculate ϵ and λ for each individual experimental group,
548 we generate 4 equations, (one for each experimental group of the form given in Eq. 1 but with different values of
549 $\delta^{15}\text{N}_{\text{diet}}$) and fit them simultaneously using least-squares regression. From this fit, we are able to obtain estimates
550 for both ϵ and λ in *B. elegans*. An inherent assumption of this approach is that all experimental groups have the
551 same ϵ -folding time and the same trophic isotope effect. We note here that we refer to the ϵ -folding time as the
552 'turnover rate' of N in corals throughout the rest of this text (e.g., Tanaka et al. 2018). Our model fit yielded a
553 trophic isotope effect, ϵ , of 3.0% with a standard error of 0.1% between coral tissue and diet. The turnover rate
554 of N (i.e. ϵ -folding time, $1/\lambda$) was 291 days with a standard error of 15 days. The four individual model equations
555 generated by our nonlinear least squares regression are presented as the dashed lines in Figure 3.

556 3.2 Effect of starvation

557 At the onset of the starvation trial, the coral tissue had an average $\delta^{15}\text{N}$ of $11.5 \pm 0.1\%$. At the end of the
558 522-day experiment, the starved group (N=15 coral individuals) had an average $\delta^{15}\text{N}$ of $12.4 \pm 0.4\%$ and the
559 frequently fed group (N=15) with a $\delta^{15}\text{N}$ of $12.7 \pm 0.1\%$ (Figure 4). The starved group was $+2.5 \pm 0.4\%$

Deleted: t

Formatted: Space Before: 4 pt

Formatted: Font color: Text 1

Deleted: specific

Formatted: Font color: Text 1

Formatted: Font color: Text 1

Formatted: Font color: Text 1

Formatted: Font color: Text 1

Formatted: Font color: Text 1

Formatted: Font color: Text 1

Deleted: T

Deleted: assumes

Formatted: Font: Not Italic, Font color: Text 1

Formatted: Font color: Text 1

Moved up [1]: In order to determine the trophic $\delta^{15}\text{N}$ offset between tissue and prey and to estimate the turnover time of the coral tissue with respect to nitrogen, we fit the data to a least-squares regression corresponding to an isotope mixing model in which describes the time-dependent evolution of tissue $\delta^{15}\text{N}$ in relation to that of the diet (Eq. 1, after Cerling et al. 2007; Ayliffe et al. 2004),
$$N = \delta^{15}\text{N}_{\text{diet}} + \epsilon e^{-\lambda t}$$
 Equation 1

The term $\delta^{15}\text{N}_{\text{diet}}$ is the value of the coral tissue at the onset of the experiment, $\delta^{15}\text{N}_{\text{diet}}$ is that of the corals' *Artemia* diet, t is the number of days since the start of the experiment, ϵ is the difference between the $\delta^{15}\text{N}$ of the diet and tissue at equilibrium, and λ is the specific nitrogen incorporation rate (d^{-1}), the inverse of which is the turnover time for N. Values of ϵ and λ were estimated by generating 4 simultaneous equations using the $\delta^{15}\text{N}$ of soft tissue and diet for the 4 treatments groups.

Deleted: Expecting the difference between coral tissue and prey $\delta^{15}\text{N}$ among experimental groups to ultimately converge, corals had evidently not reached isotopic equilibrium relative to prey by the end of the culture experiment. In order to determine the trophic $\delta^{15}\text{N}$ offset between tissue and prey and to estimate the turnover time of the coral tissue with respect to nitrogen, we fit the data to a least-squares regression corresponding to an isotope mixing model in which describes the time-dependent evolution of tissue $\delta^{15}\text{N}$... [15]

Deleted: The

Deleted: offset

Deleted: isotopic

Deleted: time

Deleted: ± 15

Deleted: ($\lambda \pm$ standard error)

Deleted: also

Deleted:

Deleted: $\delta^{15}\text{N}$

Formatted: Font color: Text 1

607 compared to its diet, statistically indistinguishable from that of the frequently fed group of $+2.8 \pm 0.1$ ‰ higher
 608 than the diet (p-value = 0.059, pairwise t-test).

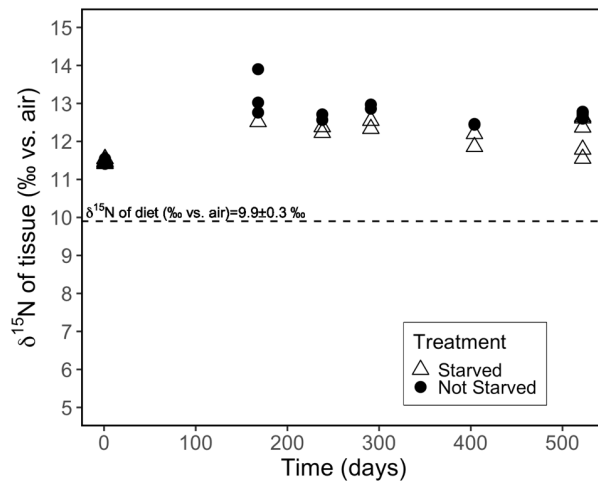


Figure 4. Evolution of the $\delta^{15}\text{N}$ of individual coral polyps fed *Artemia* nauplii ($\delta^{15}\text{N}$ 9.9 ‰) twice weekly (not starved) vs. every two weeks (starved). The analytical error associated with individual tissue $\delta^{15}\text{N}$ measurements was ± 0.2 ‰.

609 3.3 $\delta^{15}\text{N}$ comparison of field specimen polyp tissue and skeleton

610 The $\delta^{15}\text{N}$ of the soft tissue from individual *B. elegans* specimens collected live near Friday Harbor ranged
 611 between 11.2 to 13.1 ‰, averaging 12.0 ± 0.6 ‰ (Figure 5a). The soft tissue $\delta^{15}\text{N}$ differed among coral groups
 612 collected during different sampling campaigns, with higher values in spring (March 2019 and April 2021)
 613 compared to summer and fall (June 2019, September and November 2020; ANOVA $F(4) = 40.39$; p-value ≤ 0.01 ,
 614 post-hoc pairwise t-test; p-value < 0.05). The average $\delta^{15}\text{N}$ of corresponding skeletal tissue was 13.5 ± 0.7 ‰ and
 615 did not differ discernibly among sampling campaigns (ANOVA $F(2) = 0.916$; p-value = 0.431). The average

Deleted: ; Figure 4

Deleted: ¶

Formatted: Font color: Text 1

Formatted: Font color: Text 1

Formatted: Font color: Text 1

Formatted: Font color: Text 1

Formatted: Line spacing: single

Formatted: Font color: Text 1

Formatted: Left, Indent: First line: 0.5", Space Before: 8 pt, After: 4 pt, Line spacing: 1.5 lines

Deleted: .

621 difference between skeleton and soft tissue $\delta^{15}\text{N}$ ($\Delta\delta^{15}\text{N}$) among coral individuals for which both soft tissue and
 622 skeleton was measured was $1.2 \pm 0.6\%$ (Figure 5b).

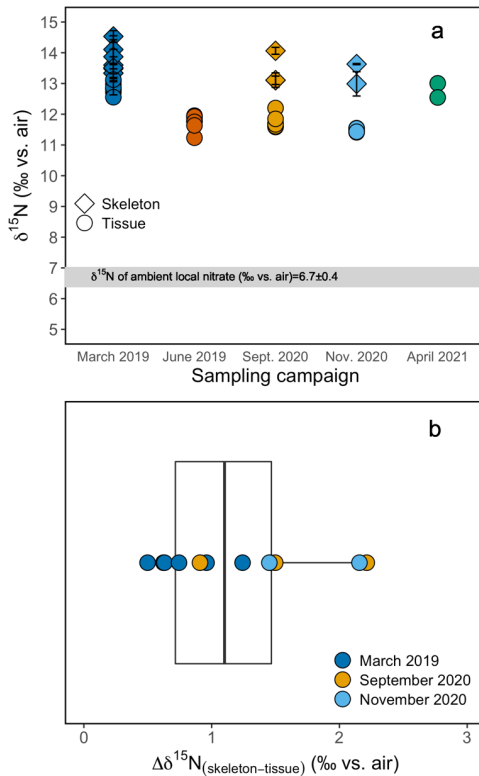


Figure 5. (a) Tissue and skeleton $\delta^{15}\text{N}$ measurements from *B. elegans* individuals collected during different sampling campaigns. Errors on skeleton data are based on replicate analyses of samples from individual polyps. (b) Boxplot of the difference between tissue and skeleton of individual *B. elegans* corals. The boxplot shows the mean, first and third quartile, maxima, and minima. Individual data points are overlaid on the plot. Colors correspond to respective sampling campaigns.

623 3.4 Regional hydrography and N isotope ratios of nitrate and plankton material

624 Hydrographic profiles recorded at stations near Friday Harbor in August 2021 showed characteristic density
 625 structures that were sensitive to tidal phase (Figure 6 a,b; Banas et al. 1999). Profiles collected during flood tide

Commented [JG1]: I find myself not understanding the lines about the "error" in the caption

Deleted: were

Deleted: ¶

Formatted: Font color: Text 1

Formatted: Font color: Text 1

Formatted: Font color: Text 1

Formatted: Font color: Text 1

Formatted: Font color: Text 1

Formatted: Font color: Text 1

Formatted: Indent: First line: 0", Space Before: 0 pt, After: 0 pt, Line spacing: single

Deleted:

Deleted: Errors on skeleton $\delta^{15}\text{N}$ are given in the text.

Deleted: tissue

Deleted: measurements of

Formatted: Font: 11 pt, Font color: Text 1

Formatted: Font: 11 pt, Font color: Text 1

Formatted: Font: 11 pt

Deleted: ¶

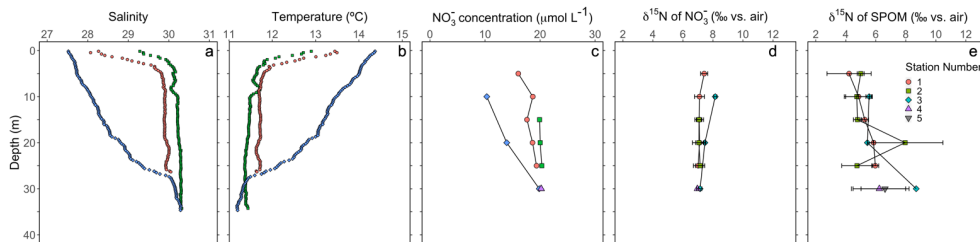
Deleted: Figure 5. (a) Tissue and skeleton $\delta^{15}\text{N}$ measurements from *B. elegans* individuals collected during different sampling campaigns. Errors on skeleton $\delta^{15}\text{N}$ are given in the text. Errors on tissue data are based on measurements of replicate samples. (b) Boxplot of the difference between tissue and skeleton of individual *B. elegans* corals. The boxplot shows the mean, first and third quartile, maxima, and minima. Individual data points are overlaid on the plot. Colors correspond to respective sampling campaigns. ¶

Formatted: Font color: Text 1

637 (collected between 11:40 and 14:20 on August 2, 2021), were relatively well-mixed (salinity 30, temperature
 638 11.8°C), with fresher and warmer water restricted to the near surface (≤ 5 m), whereas ebb-tide profiles (collected
 639 at 9:00 on August 2, 2023) showed a progressive decrease in salinity from 30 to 27 and a corresponding increase
 640 in temperature from 11.8°C at 35 m to 14.5°C at the surface.

641 Nitrate concentrations were nearly uniform with depth during flood tide ($\sim 20 \mu\text{mol L}^{-1}$), decreasing slightly at
 642 5 m, whereas during ebb tide nitrate concentrations decreased progressively from 20 to $10 \mu\text{mol L}^{-1}$ between 30
 643 and 10 m (Figure 6c). Nitrate concentrations in samples collected during the other sampling campaigns ranged
 644 from 12 to $32 \mu\text{mol L}^{-1}$, and appeared generally higher at stations visited during the September and November
 645 2020 campaigns compared to those in April and August 2021 (Figure S6).

646 Depth profiles collected in August 2021 revealed uniform nitrate $\delta^{15}\text{N}$ values of $\sim 7 \text{‰}$ at 30 m among
 647 profiles. In well-mixed profiles, nitrate $\delta^{15}\text{N}$ increased slightly to 7.5 ‰ above 10 m. In stratified profile, nitrate
 648 $\delta^{15}\text{N}$ increased progressively to 8.2 ‰ at 10 m (Figure 6d). Among all sampling campaigns, the $\delta^{15}\text{N}$ of nitrate
 649 ranged from 6.1 ‰ to 8.2 ‰, with median values of $6.8 \pm 0.4 \text{‰}$ (Figure 7a). The relationship between nitrate
 650 $\delta^{15}\text{N}$ and nitrate concentration in August 2021 was fit to a closed-system Rayleigh distillation model (Mariotti et
 651 al. 1981), suggesting a nitrate assimilation isotope effect of $1.5 \pm 0.1 \text{‰}$ (Figure 8).



652 **Figure 6.** Depth profiles during the August 2021 sampling campaign of (a) salinity, (b) temperature, (c) nitrate
 653 concentration, (d) the $\delta^{15}\text{N}$ of nitrate for analytical replicates and (e) the $\delta^{15}\text{N}$ of SPOM of replicate samples (n
 654 ≥ 2). Green and red symbols correspond to flood tide (collected between 11:00am and 2:00pm on August 2,
 655 2021), blue symbols correspond to ebb tide (collected at 9:00am on August 3, 2021).

652 The $\delta^{15}\text{N}$ of SPOM collected at depths above 35 m near Friday Harbor during the different sampling
 653 campaigns ranged from 1.6 to 11.7 ‰, averaging $5.7 \pm 1.7 \text{‰}$ (Figure 7b). Values were lowest for the four
 654 samples collected in April ($4.4 \pm 0.4 \text{‰}$), and highest for the four samples collected in September and November
 655 ($6.2 \pm 2.6 \text{‰}$), although these trends may be an artifact of the low data density in April ($n = 4$) and Sept./Nov. (n
 656 $= 5$) relative to August 2021 ($n = 29$), at which time the observed range of $\delta^{15}\text{N}$ subsumed that in the other two

Formatted: Font color: Text 1

Formatted: Font color: Text 1

Deleted: at 30 m

Formatted: Font color: Text 1

Formatted: Font color: Text 1

Deleted: ¶

Formatted: Font color: Text 1

Formatted: Line spacing: single

Formatted: Font color: Text 1

Formatted: Font color: Text 1

Deleted: spring

Deleted: autumn

Deleted: spring

Deleted: autumn

664 campaigns. Values did not differ coherently with depth in August 2021, although any potential depth structure
665 was obscured by the large variability among sample replicates (Figure 6e).

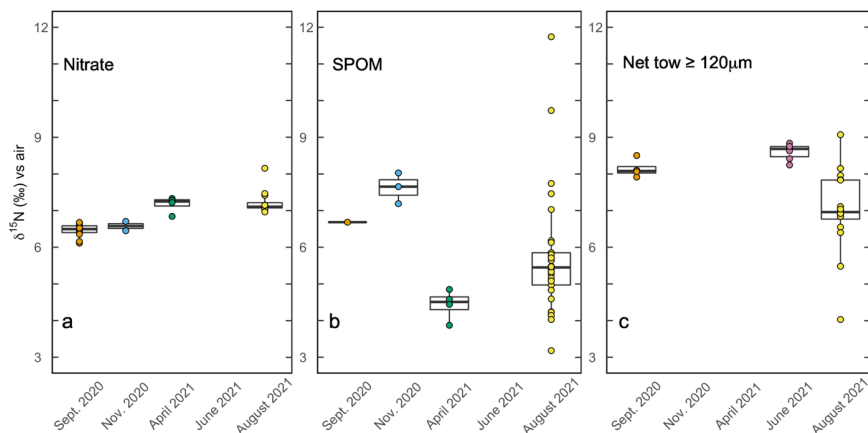


Figure 7. Boxplots of aqueous and particulate N pools at respective sampling times. (a) The $\delta^{15}\text{N}$ of nitrate from samples above 30 m collected during respective sampling campaigns. (b) The $\delta^{15}\text{N}$ of suspended particulate organic matter (SPOM) at sites near Friday Harbor during respective sampling campaigns. (c) The $\delta^{15}\text{N}$ of net tows ($\geq 120\ \mu\text{m}$ mesh size) conducted during respective sampling campaigns.

666 The $\delta^{15}\text{N}$ of material collected in net tows (120 μm mesh size) during sampling campaigns in September 2020,
667 and June 2021 ranged between 7.9 to 8.8 ‰ (Figure 7c). Material collected in net tows of 80 μm and 150 μm
668 mesh size in August 2021 and separated by size class post-collection revealed a coherent $\delta^{15}\text{N}$ increase with size
669 class (Figure 7c; Figure 9). The $\geq 80\ \mu\text{m}$ size class had a mean $\delta^{15}\text{N}$ of $6.0 \pm 0.3\ \text{‰}$ whereas that $\geq 500\ \mu\text{m}$ had an
670 average $\delta^{15}\text{N}$ of $8.0 \pm 0.8\ \text{‰}$, which was significantly greater than the $\delta^{15}\text{N}$ of the other size classes (ANOVA, p-
671 value < 0.05).

672 4. Discussion

673 This study of *B. elegans* provides novel constraints on the trophic ecology of scleractinian CWCs. Foremost,
674 our observations of *B. elegans* collectively suggest that the relatively large global $\delta^{15}\text{N}$ offset of 8-9 ‰ between
675 CWC skeletal tissue and the $\delta^{15}\text{N}$ of PON exported from the surface ocean is neither explained by a large
676 difference between tissue and skeleton $\delta^{15}\text{N}$, nor by an unusually large trophic isotope effect. Further, controlled

Formatted: Font color: Text 1

Formatted: Font color: Text 1

Formatted: Font color: Text 1

Formatted: Font color: Text 1

Formatted: Line spacing: 1.5 lines

Formatted: Font color: Text 1

Formatted: Space Before: 10 pt, Line spacing: 1.5 lines

Formatted: Left, Indent: First line: 0.25", Space Before: 4 pt, After: 4 pt, Line spacing: 1.5 lines

677 feeding experiments yielded direct estimates of the trophic isotope effect and the corresponding N turnover **rate**
 678 of *B. elegans* soft tissue. Examination of soft tissue $\delta^{15}\text{N}$ of wild specimens in relation to regional hydrography
 679 and food web components near Friday Harbor **leads** us to conclude that *B. elegans* feeds predominantly metazoan
 680 zooplankton prey, implicating more than one trophic transfer between **exported** PON and coral soft tissue. We
 681 contextualize our findings to existing studies of CWC trophic ecology and discuss the implications of considering
 682 a two-level trophic transfer for paleo-reconstructions of ocean N cycling using *B. elegans* and CWCs **more**
 683 generally.

Deleted: time
Deleted: compels
Formatted: Font color: Text 1
Formatted: Font color: Text 1
Formatted: Font color: Text 1
Formatted: Font color: Text 1

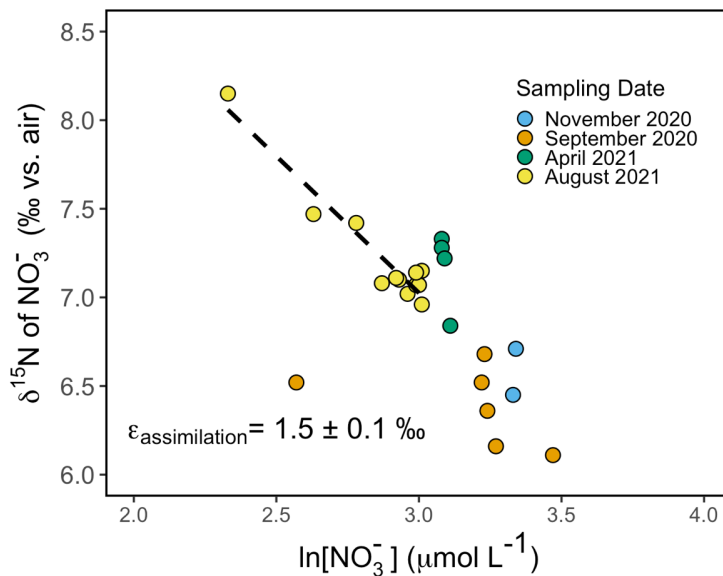


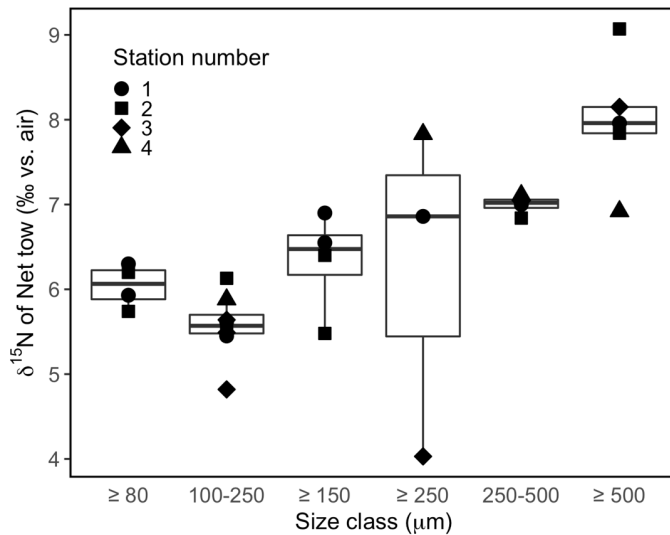
Figure 8. Rayleigh plot of nitrate $\delta^{15}\text{N}$ vs. \ln of nitrate concentration for samples collected from the surface to 40 m around Friday Harbor. The isotope effect of $\sim 1.5 \pm 0.1$ ‰ corresponds to the slope of the best fit linear regression line for the August 2021 data, $\delta^{15}\text{N}_{\text{NO}_3} = 11.7 - 1.5 \ln [\text{NO}_3^-]$.

Formatted: Font: 11 pt, Font color: Text 1
Formatted: Font: 11 pt, Font color: Text 1
Formatted: Font: 11 pt, Font color: Text 1
Formatted: Font: 11 pt, Font color: Text 1
Formatted: Font: 11 pt, Font color: Text 1
Formatted: Font: 11 pt, Font color: Text 1
Formatted: Font: 11 pt, Font color: Text 1
Formatted: Font: 11 pt, Font color: Text 1
Formatted: Font: 11 pt, Font color: Text 1
Formatted: Font: 11 pt, Font color: Text 1
Deleted: queried
Formatted: Font color: Text 1
Formatted: Font color: Text 1

684 4.1 Culture experiments revealed a normal trophic isotope effect
 685 We **investigated** whether the large difference in $\delta^{15}\text{N}$ between PON export from the surface and coral
 686 skeleton-bound $\delta^{15}\text{N}$ (8-9 ‰) observed by Wang et al. (2014) could arise from an unusually large trophic level
 687 offset specific to CWCs. The long-term feeding experiment of *B. elegans* polyps revealed a ‘normal’ trophic

691 isotopic offset between coral tissue and diet of $\epsilon = +3.0 \pm 0.1 \text{ ‰}$. This value conforms to the expected range of
 692 $+3.4 \pm 1.1 \text{ ‰}$ for a single trophic level offset in $\delta^{15}\text{N}$ (Minagawa and Wada, 1984).

693



Deleted: (
 Deleted: of
 Deleted: - a value that
 Deleted:)

Figure 9. Boxplots of net tow material collected above 30 m in August 2021, separated by size class.

694

695 To support the above conclusion, we assess the assumptions inherent to the isotope mixing model (Eq. 1)
 696 used to derive ϵ and the corresponding nitrogen turnover rate from our culture data. First, the model only
 697 accounts for the turnover of a single pool of N, requiring the assumption that all N in the coral polyp tissues
 698 equilibrate at the same rate. This notion is unlikely to be wholly accurate, as fluxes of N may vary among tissue
 699 types. However, given the relatively low resolution of our sampling over the course of the culture experiments
 700 (necessary due to constraints on numbers of total samples) we are unable to extend our model to one with
 701 multiple pools (e.g. as in Ayliffe et al. 2004). As soft tissues of individual coral polyps were homogenized, we
 702 suggest that the $\delta^{15}\text{N}$ values and corresponding estimate of ϵ thus represent the average of soft tissues with
 703 potentially different turnover rates. The estimates of ϵ and N turnover rate further rely on the assumption that the

Formatted: Font color: Text 1
 Formatted: Line spacing: single
 Formatted: Font color: Text 1
 Formatted: Font color: Text 1
 Formatted: Line spacing: 1.5 lines
 Deleted: turnover
 Deleted: turnover time
 Deleted: ies

Formatted: Font color: Text 1
 Deleted: s
 Formatted: Font color: Text 1

712 nutritional quality of the respective diets among treatments was equivalent, as trophic isotope effects can be
713 sensitive to food type. Diets low in protein can be associated with greater ϵ values due to internal recycling of
714 nitrogen (Adams and Sterner, 2000; Webb et al., 1998). For instance, locusts fed a low protein diet were enriched
715 5.1 ‰ from their diet, compared to 2.3‰ for those fed a high protein diet (Webb et al., 1998). Conversely, a
716 compilation of studies of various metazoan consumers raised on controlled diets suggests that high protein diets
717 generally result in higher trophic isotope effects (~3.3 ‰) compared to more herbivorous diets (~2.2 ‰), a
718 dynamic ascribed to higher rates of N excretion to assimilation in consumers fed high protein diets (McCutchan
719 Jr et al., 2003). ~~As noted in Table S3 and in Section 2.3.1, our *Artemia* prey had similar C:N ratios among~~
720 ~~treatments, in line with our model treatment. Finally, our model assumes that N turnover was dominated by~~
721 ~~metabolic tissue replacement, rather than net growth, consistent with the observation that adult *B. elegans* growth~~
722 ~~is slow (Gerrodette 1981).~~

723 Equation 1 could be invalidated ~~if the corals can access nutritional N sources other than N in *Artemia*, given~~
724 ~~that the model assumes that *Artemia* are the only source of N to corals in our experiment.~~ Biological N₂ fixation
725 and chemoautotrophy have been detected in association with CWC holobionts, providing some N nutrition to the
726 corals (Middelburg et al., 2016). Our trophic isotope effect estimate was in the range expected for a single trophic
727 transfer, arguably suggesting that N₂ fixation, if occurring, ~~was not a substantial contribution~~ to the corals'
728 nutrition; it would otherwise result in a lower value of ϵ given a $\delta^{15}\text{N}$ contribution of -1 to 0 ‰ (Carpenter et al.
729 1997). That the trophic isotope effect of the poorly fed corals did not differ from that of corals that were well-fed
730 also argues for no sources of N additional to the *Artemia*, as starved corals would presumably increase their
731 reliance on said source. In a related vein, N recycling between the *B. elegans* specimens and potential microbial
732 symbionts (e.g. Middelburg et al. 2016) could also dampen the trophic isotope effect relative to the *Artemia* prey
733 and yield an over-estimate of soft tissue ~~turnover rate for N~~. The normal trophic isotope effect ~~indicated here~~
734 ~~suggests~~ a modest role of N retention and recycling by microbial symbionts, in contrast to tropical symbiotic
735 corals wherein bacterial symbionts promote substantial N retention and recycling, and consequently lower trophic
736 isotope effects (Tanaka et al. 2018). Finally, the validity of our estimates could be sensitive to differences in
737 feeding rates, which can influence the rate of N turnover of tissues (Martinez del Rio and Carleton, 2012; Rangel
738 et al., 2019). Corals were fed at identical times among treatments, at a relatively high feeding rate (Crook et al.,
739 2013). However, given the limited number of studies on feeding in *B. elegans*, it is difficult to compare our
740 feeding strategy and that of this species' natural environment. Overall, we consider that the mixing model

Deleted: To avoid diet quality confounding our estimates, we verified that the...

Deleted: ensuring a similar nutritional value

Deleted: The end-member mixing represented by

Deleted: also

Deleted: given

Deleted: additional to

Deleted: the

Deleted: s

Deleted: contributed modestly

Deleted: 2016)

Formatted: Not Highlight

Deleted: turnover

Deleted: evinced

Deleted: argues for

Deleted: to encourage growth

756 described by Equation 1 is appropriate to derive the first-order trophic isotope effect and turnover rate of *B.*
757 *elegans*.

758 Changes in metabolism due to underfeeding or prolonged fasting have the potential to increase trophic-level
759 isotope offsets due to increased protein metabolism (Adams and Sterner, 2000). For instance, extensive amino
760 acid recycling in overwintered adult insect larvae was cited to explain trophic isotope effects upward of 10‰
761 (Scrimgeour et al., 1995). A meta-analysis on the effects of starvation on consumer $\delta^{15}\text{N}$ revealed that starvation
762 generally led to increased organism $\delta^{15}\text{N}$ by an average of 0.5 ‰, up to 4.3 ‰ (Doi et al., 2017). This dynamic
763 was documented for the tropical symbiotic coral *Stylophora phistillata*, where heterotrophically starved corals
764 were enriched in $\delta^{15}\text{N}$ by ~0.5 ‰ compared to frequently fed corals (Reynaud et al., 2009). The trophic isotope
765 offset of *B. elegans* soft tissue relative to its diet, ϵ , was not discernibly influenced by near starvation; that of
766 corals fed once every other week was similar to that of corals fed twice a week – in spite of visible signs of stress
767 among the former, including relatively more sluggish feeding (Figure S7) and thinner soft tissue (data not
768 shown). Deep sea coral reefs are often highly productive environments with high levels of biodiversity,
769 commensurate with a relatively high food supply (Duineveld et al., 2007; 2004; Genin et al., 1986; Roberts et al.,
770 2006; Soetaert et al., 2016; Thiem et al., 2006; Cathalot et al. 2015). Nevertheless, periodicity and spatial
771 heterogeneity in the food supply of CWC reefs implicate periods of lower food density (e.g., Duineveld et al.
772 2007). High currents, downwelling and/or vertically migrating zooplankton temporally boost the export of
773 surface organic matter to the seabed, creating ‘feast’ conditions, interspersed with ‘famine’ periods during the
774 non-productive season (Maier et al. 2023). Regardless, our trials suggest that starvation, if pertinent to CWC
775 communities, does not result in greater-than-expected trophic isotope offsets, at least for *B. elegans*.

776 4.2 Turnover rate for *B. elegans*

777 We report the first estimate of the nitrogen turnover for a non-symbiotic cold-water coral of 291 ± 15 days
778 for *B. elegans* soft tissue. This value falls within the range of existing estimates for tropical symbiotic corals.
779 Pulse-chase experiments with ^{15}N -nitrate conducted with fragments of the tropical symbiotic coral *Porites*
780 *cylindrica* yielded a N turnover time of 370 days, and of 210 days for the tropical symbiotic coral *Acropora*
781 *pulchra* (Tanaka et al. 2006; 2018). These relatively long turnover times are attributed to the recycling and
782 retention of N within the coral-symbiont system in nutrient-deplete ecosystems. In comparison, the corresponding
783 carbon turnover in *A. pulchra* was 18 days – compared to 210 days for N – because the system is ultimately N
784 limited (Tanaka et al., 2006). Tanaka et al. (2018) inferred that the N turnover in *P. cylindrica* would be
785 substantially faster than 370 days without symbionts, on the order of 56 days based on estimates of polyp-specific

Deleted: time

Deleted: The extent to which CWCs experience significant periods of starvation *in-situ* is unclear.

Formatted: Font color: Text 1

Formatted: Font color: Text 1

Formatted: Font color: Text 1

Deleted: ; Kiriakoulakis et al. 2007

Deleted: time

Deleted: of

Formatted: Font: Italic

Formatted: Font color: Text 1

792 N uptake rates. Nevertheless, the N turnover estimated for the tropical symbiotic coral *Porites lutea* was notably
793 shorter than *A. pulchra* and *P. cylindrica*, on the order of 87 days (Rangel et al., 2019), implicating different N
794 nutritional strategies among symbiotic coral groups and/or ecosystems. The N turnover for *B. elegans* estimated
795 here is of the same order as but still longer than that for tropical symbiotic corals suggesting that cold-water
796 species have lower metabolic and growth rates compared to tropical symbiotic species, although efficient N
797 recycling has also been documented previously in cold-water corals (Middelburg et al. 2016). The slower
798 turnover of CWCs relative to their symbiotic tropical counterparts may reflect the lower temperatures of the
799 former's habitats (Miller, 1995; Thomas and Crowther 2015).

800 Constraints on N turnover also allow for calibration of the temporal resolution that is achievable with the
801 CWCs $\delta^{15}\text{N}$ proxy for marine N cycling. Corals are constantly accreting skeleton, such that coral proxies have the
802 potential to provide annual resolution (e.g. Adkins et al. 2004). In theory, a rapid N turnover in CWC could
803 record seasonal changes in regional N dynamics. A turnover time of 291 ± 15 days for N in *B. elegans* soft tissue,
804 however, signifies that the $\delta^{15}\text{N}$ of coral skeleton is unlikely to provide a faithful record of seasonal differences in
805 the $\delta^{15}\text{N}$ of the coral diet. Moreover, the turnover of the pool of N that sources the skeletal tissue may be different
806 from that of bulk tissue, and thus decoupled from the soft tissue turnover rate. We suggest that CWCs can likely
807 record changes in their diet on annual or longer timescales, compatible with the ability to date CWC with
808 subdecadal resolution (Adkins et al. 2004).

809 4.3 Soft tissue vs. skeleton $\delta^{15}\text{N}$

810 A large biosynthetic $\delta^{15}\text{N}$ offset between the coral soft tissue and its skeleton could conceivably account for a
811 large $\delta^{15}\text{N}$ offset between coral skeleton-bound organic matter and N of export that is not explained by single
812 trophic level enrichment of $\sim 3\%$. However, the mean difference between soft tissue and skeleton-bound $\delta^{15}\text{N}$
813 among *B. elegans* specimens collected at Friday Harbor was relatively modest, on the order of $+1.2\%$, ranging
814 between $+0.5$ and $+2.2\%$. The observed range was dictated primarily by the variability in the $\delta^{15}\text{N}$ of the coral
815 soft tissue, as skeleton-associated $\delta^{15}\text{N}$ values were relatively invariant among specimens sampled from different
816 locations and field seasons, likely due to the fact that the amount of skeleton analyzed represented multiple
817 years of growth. The amount of skeleton-bound organic N is small relative to aragonite mass ($2\text{--}5\ \mu\text{mol N per g}$
818 of skeleton in our samples), such that homogenization of 50-100 mg aragonite fragments may alias seasonally-
819 driven variability in skeletal $\delta^{15}\text{N}$. Soft tissue values in spring were $\sim 1.5\%$ higher than in summer and fall, such
820 that they appeared to record seasonal changes in diet (Figure 5a). In this regard, the asymptotic nature of the two
821 end-member isotope mixing model (Eq. 1) renders *B. elegans*'s soft tissue sensitive to seasonal changes in prey

Deleted: as

Deleted: and/or metabolisms

Deleted:

Formatted: Font: Italic, Font color: Text 1

Formatted: Font color: Text 1

Deleted: time

Formatted: Font color: Text 1

Deleted: ,

Deleted: worth

Formatted: Font color: Text 1

Formatted: Font color: Text 1

Formatted: Font color: Text 1

828 $\delta^{15}\text{N}$, but not likely to reach isotopic equilibrium on seasonal timescales - given an N turnover of ~291 days, as
829 discussed above. Seasonal variations in the $\delta^{15}\text{N}$ of the food source of *B. elegans* near Friday Harbor could arise
830 from corresponding differences in the $\delta^{15}\text{N}$ of nitrate entrained to the surface driven by seasonal hydrographic
831 variability around San Juan archipelago, in the extent of surface nitrate consumption, in food web structure, or
832 from some combination of these. The data density among all but the August 2021 sampling campaign is too
833 sparse to be conclusive in this regard. Otherwise, the observed differences in soft tissue $\delta^{15}\text{N}$ may result from
834 spatial heterogeneity in food source $\delta^{15}\text{N}$ among the different collection sites visited for respective campaigns at
835 Friday Harbor.

Formatted: Font color: Text 1

836 As documented here for *B. elegans*, the $\delta^{15}\text{N}$ difference between coral tissue and skeleton appears to be
837 modest among various scleractinian coral species. Specimens of the symbiotic tropical coral *Porites lutea* showed
838 a $\delta^{15}\text{N}$ offset of +1.1 ‰ between skeleton and soft tissue, whereas the symbiotic tropical coral *Favia stelligera*
839 revealed an insignificant offset of -0.1 ‰ (Erlor et al., 2015). Similarly, no offset was observed for proteinaceous
840 cold-water corals of the genus *Lepidisis* collected off Tasmania (Sherwood et al., 2009), whereas an offset of -1.9
841 ± 0.8 ‰, was reported for cold-water proteinaceous corals of the genus *Primnoa* from the Gulf of Alaska,
842 *Isadella* from the Central California Margin, and *Kulamanamana* from the North Pacific Subtropical Gyre
843 (McMahon et al., 2018). Conversely, a study of numerous species of both symbiotic and non-symbiotic corals
844 reported a +4 ‰ offset between the skeletal organic matrix and soft tissue among the non-symbiotic corals
845 specifically, but no difference among the symbiotic corals (Muscatine et al., 2005), suggesting that biosynthetic
846 offsets may occur for certain CWC species or conditions.

847 4.4 Implications for components of CWC diet

848 Cold water corals are considered opportunistic feeders, ingesting whatever is available in the water column
849 (Mortensen, 2001; Freiwald, 2002; Duineveld et al. 2004; 2007; Kiriakoulakis et al. 2005; Carlier et al. 2009;
850 Dodds et al. 2009; van Oevelen et al. 2009). They are reported to feed on zooplankton (Kiriakoulakis et al., 2005;
851 Naumann et al., 2011), including microzooplankton (Houlbrèque et al. 2004), on phytoplankton and
852 phytodetritus, including the bacterial fraction of phytodetritus (Maier et al., 2020; Houlbrèque et al. 2004),
853 dissolved organic matter (Mueller et al., 2014; Ferrier 1991; Al-Moghrabi et al. 1993; Hoegh-Guldberg &
854 Williamson 1999; Houlbrèque et al. 2004; Grover et al. 2008), and the CWC holobiont has been observed to
855 display biological N_2 fixation and chemoautotrophy (Middelburg et al. 2016). While it is clear that corals may be
856 able to consume a variety of components within the food web, the soft tissue $\delta^{15}\text{N}$ of *B. elegans* specimens
857 collected at Friday Harbor averaged 12.0 ‰, signifying that they fed on material with a $\delta^{15}\text{N}$ of approximately

Deleted: C

Deleted: g

Formatted: Font color: Text 1

Formatted: Indent: First line: 0", Line spacing: 1.5 lines

Deleted: 2012.

Deleted: v

Formatted: Not Highlight

Formatted: No underline, Font color: Text 1

Formatted: Font color: Text 1

Formatted: No underline, Font color: Text 1

Formatted: Font color: Text 1

Formatted: No underline, Font color: Text 1

Formatted: Font color: Text 1

Formatted: No underline, Font color: Text 1

Formatted: Font color: Text 1

Moved (insertion) [3]

862 9.0 ‰ – accounting for a normal trophic offset relative to their diet (3 ‰) confirmed by our culture experiment
 863 results. Here, we seek to determine the primary nutrition source for *B. elegans* at Friday Harbor by comparing the
 864 $\delta^{15}\text{N}$ of these corals' expected diet with measured $\delta^{15}\text{N}$ of different food web components including SPOM and
 865 net tow material.

866 We first explore whether the SPOM fraction of the food web was the dominant component of *B. elegans*' diet
 867 at Friday Harbor. SPOM is operationally defined as the particulate material retained onto glass fiber filters (GF/F,
 868 0.7 μm nominal pore size) from filtered aqueous samples. At the ocean surface, including at the stations near
 869 Friday Harbor, SPOM is generally dominated by phytoplankton material. At the ocean subsurface, below the
 870 euphotic zone, SPOM derives from organic material exiting the ocean surface, but is considered a distinct pool
 871 from the ballasted sinking PON collected in sediment traps. The $\delta^{15}\text{N}$ of SPOM typically increases with depth,
 872 with the steepest gradient across the 100-300 m depth interval, reaching upwards of ~4-5 ‰ in the ocean
 873 subsurface, which are higher values than the corresponding sinking particles at abyssal depths due to recycling
 874 and remineralization (Altabet, 1988; Casciotti et al., 2008; Saino and Hattori, 1987). Wang et al. (2014) reasoned
 875 that because the $\delta^{15}\text{N}$ of SPOM is approximately one trophic level lower than that of the N preserved in skeletons of
 876 the deep-dwelling (deeper than ~500 m) CWC *Desmophyllum dianthus*, and because suspended particles are the
 877 most abundant form of small particles in the deep ocean, cold-water corals must feed predominantly on SPOM.
 878 However, SPOM collected in the upper 30 meters near Friday Harbor was 5.7 ± 1.7 ‰, which is ~6 ‰ lower
 879 than *B. elegans* soft tissue, a difference greater than expected for a single trophic level. Thus, the SPOM at Friday
 880 Harbor was evidently not the predominant food source for *B. elegans* growing in this depth interval.

881 Additionally, it has been suggested that CWCs can assimilate dissolved organic nitrogen (DON) (Gori et al.,
 882 2014). We do not have $\delta^{15}\text{N}$ DON measurements from our field study. However, we do not expect the potential
 883 assimilation of DON to explain the elevated $\delta^{15}\text{N}$ of organic tissue that was observed. There are two components
 884 of marine DON, refractory and labile (Bronk et al. 2002), which have different $\delta^{15}\text{N}$ (Knapp et al. 2018). At
 885 Friday Harbor, we don't know the partitioning of the $\delta^{15}\text{N}$ between these pools, but even if we did, the labile
 886 fraction (which would presumably be the pool available to corals) is expected to converge on the $\delta^{15}\text{N}$ value of
 887 SPOM (Bronk et al., 2002, Sigman and Fripiat 2019 their Fig. 4; Knapp et al., 2018, Zhang et al., 2020), given
 888 that the most recently produced DON is generally most labile. As a result, consumption of DON would not
 889 explain the high $\delta^{15}\text{N}$ of coral organic tissue.

890 Instead, we suggest that the relatively high $\delta^{15}\text{N}$ of ~12 ‰ of *B. elegans* soft tissue at Friday Harbor results
 891 from these corals deriving nutrition predominantly from larger metazoan zooplankton. Indeed, this is supported
 892 by a comparison of the $\delta^{15}\text{N}$ coral tissue and the $\delta^{15}\text{N}$ of the largest size class of net tow material ($\geq 500 \mu\text{m}$) of

- Deleted: incubation
- Deleted: .
- Moved up [3]: soft tissue $\delta^{15}\text{N}$ of *B. elegans* specimens collected at Friday Harbor averaged 12.0 ‰, signifying that they fed on material with a $\delta^{15}\text{N}$ of approximately 9.0 ‰ – accounting for a normal trophic offset relative to their diet (3 ‰).
- Deleted: ¶
There is a lack of consensus, however, regarding which components of the food web dominate their diets. The
- Formatted: Font color: Text 1
- Deleted: defined as
- Deleted:
- Deleted:
- Deleted: in the ocean subsurface
- Deleted: can be
- Deleted: heavier
- Formatted: Font color: Text 1
- Formatted: Font color: Text 1
- Deleted:
- Formatted: Font color: Text 1
- Deleted: *D. dianthus*
- Formatted: Font color: Text 1
- Deleted: X ‰ (JOSIE, CAN YOU PLEASE, PROVIDE THE ACTUAL VALUE HERE
- Deleted:), WHICH IS
- Formatted: Not Highlight
- Deleted: T
- Formatted: Font color: Text 1
- Formatted: (... [16])
- Formatted: Font: 11 pt, Font color: Text 1
- Deleted: A more parsimonious explanation to account for the
- Formatted: Font color: Text 1
- Formatted: Font color: Text 1
- Formatted: Font color: Text 1
- Formatted: Line spacing: 1.5 lines
- Deleted: is that they derived
- Formatted: Font color: Text 1
- Deleted: A direct positive relationship between
- Deleted:
- Deleted: of material collected in net tows and particle size (... [17])
- Formatted: Font color: Text 1

921 $8.0 \pm 0.8 \text{ ‰}$. This is the only component of the organic matter nitrogen budget that is offset from the coral tissue
922 by $\sim 3.5 \text{ ‰}$, consistent with one trophic level transfer. Additionally, the net tow material had a molar C:N ratio of
923 4.4 ± 0.6 , compared to 6.5 ± 2.2 for the SPOM (Figure S8), suggesting a dietary preference for metazoan
924 zooplankton would provide higher protein content and nutritional density for these corals (Adams and Sterner,
925 2000).

926 Despite evidence for zooplankton as the main dietary source for *B. elegans* at Friday Harbor, we
927 acknowledge that this feeding strategy may not apply for corals of other species living in habitats that are
928 hundreds to thousands of meters deep. As pointed out in a recent review (Maier et al. 2023), the presence of
929 CWC reefs in the food-limited deep ocean appears paradoxical, and it is not likely that the food available to
930 corals at Friday Harbor looks identical to food available to corals living at $>1000 \text{ m}$ water depth. Indeed, Maier et
931 al. 2023 suggest that the biodiversity and productivity of CWC reefs in the deep sea are supported by a number of
932 processes such as CWC's ability to consume a range of dietary components (DOM, bacterioplankton, inorganic
933 resources such as inorganic C and ammonium), efficient resource recycling, and their ability to align their
934 feeding strategies and growth with fluctuations in food availability. While we cannot speculate about the flux of
935 DOM to corals living at $>1000 \text{ m}$ depth, the $\delta^{15}\text{N}$ of deep DOM has a uniform value of $\sim 5 \text{ ‰}$, which cannot
936 explain the high $\delta^{15}\text{N}$ of CWCs (see Sigman and Fripiat, 2019).

937 Maier et al. (2023) and references therein highlight that most deep CWC reefs occur in regions with higher-
938 than-average annual primary productivity, indicating that these CWC reefs are sustained by inputs of high energy
939 to the system, where there is also evidence for the presence of vertically migrating zooplankton. The vertically
940 migrating zooplankton have been found near both relatively shallow ($<200 \text{ m}$, Duineveld et al. 2007, Garcia-
941 Herrera et al., 2022) and deep ($\sim 1000 \text{ m}$, e.g. Carlier et al. 2009) CWC reefs. Moreover, there are a number of
942 other independent studies that reveal a single trophic level offset between the $\delta^{15}\text{N}$ of zooplankton prey and the
943 $\delta^{15}\text{N}$ soft tissue of asymbiotic scleractinian corals at specific sites (Duineveld et al., 2004, Sherwood et al. 2005;
944 2008; 2009; Carlier et al., 2009; Hill et al., 2014; Maier et al., 2020). Given the 'normal' trophic level offset
945 reported for CWCs in our laboratory culture experiment, these published observations underscore that
946 zooplankton could be a dominant dietary component of corals other than *B. elegans* as well. Additional evidence
947 from lipid biomarkers corroborates the assertion that deep-dwelling CWC species such *Lophelia pertusa*
948 (recently re-classified as *Desmophyllum pertusum*) and *Madrepora oculata* feed predominantly on metazoan
949 zooplankton (Dodds et al., 2009; Kiriakoulakis et al., 2005; Naumann et al. 2015). Some deep-dwelling CWCs
950 (*Desmophyllum pertusum*, *Madrepora oculata*, *Dendrophyllia cornigera*) exhibit prey preference for larger

Deleted: X ‰ (JOSIE, CAN YOU PLEASE, PROVIDE THE ACTUAL VALUE HERE as well)

Deleted: clearly shows an offset consistent with one trophic transfer, whose $\delta^{15}\text{N}$ was ($\sim 3.5 \text{ ‰}$) lower than coral soft tissue – approximating a single trophic transfer.

Deleted: OM

Deleted: At Friday Harbor

Formatted: Font color: Text 1

Deleted: support

Deleted: in the former

Formatted: Font color: Text 1

Formatted: Font color: Text 1

Deleted: in

Deleted: ,

Formatted: Font color: Text 1

Formatted: Font color: Text 1

Formatted: Font color: Text 1

Deleted: activity

Formatted: Font: (Default) +Body (Times New Roman)

Formatted: Font: (Default) +Body (Times New Roman), 11 pt

Formatted: Font: (Default) +Body (Times New Roman), 11 pt

Formatted: Font: (Default) +Body (Times New Roman), 11 pt

Formatted: Font: (Default) +Body (Times New Roman), 11 pt

Formatted: Font: (Default) +Body (Times New Roman), 11 pt

Formatted: Font: (Default) +Body (Times New Roman), 11 pt

Formatted: Font: (Default) +Body (Times New Roman)

Deleted: Nevertheless,

Formatted: Font: Italic

Deleted: s

965 zooplankton (Da Ros et al. 2022), suggesting that zooplankton prey are an essential component of their diet.
966 Indeed, an exclusive diet of phytodetritus (Maier et al. 2019) and the exclusion of zooplankton from diet
967 (Naumann et al. 2011) led to decreases in coral metabolism. More fundamentally, the shared traits of tentacles
968 and nematocysts are evidence of a predatory life strategy, indicating that zooplankton are an important food
969 source for corals (Lewis and Price, 1975; Sebens et al., 1996). The coral morphology of *B. elegans* and that of
970 other cold water scleractinian corals is consistent with an adaptation for the capture of prey of a commensurate
971 size (Fautin, 2009). Correspondingly, *D. dianthus* is considered to be a generalized zooplankton predator that can
972 prey on medium to large copepods and euphysiids (Höfer et al., 2018). In contrast, gorgonian corals do not
973 capture naturally occurring zooplankton and have a correspondingly low density of nematocysts (Lasker 1981).
974 In summary, while our data cannot directly indicate that all CWCs, including the deep-dwelling ones, derive their
975 primary nutrition from zooplankton, the results of our trophic experiment and field study (when evaluated in the
976 context of the published literature) suggest that it may be important to consider metazooplankton as a significant
977 component of CWC diet, and that CWC $\delta^{15}\text{N}$ is likely to be sensitive to food web dynamics. We discuss the
978 implications of these suggestions further in the sections below.

979 4.5 Does coral-bound $\delta^{15}\text{N}$ reflect surface ocean processes at Friday Harbor?

980 The effectiveness of coral skeleton-bound $\delta^{15}\text{N}$ as an archive to reconstruct past ocean N cycling depends on
981 its ability to record the $\delta^{15}\text{N}$ of the surface PON export. In turn, the $\delta^{15}\text{N}$ imparted to the phytoplankton
982 component of surface particles, from which PON export derives, is highly dependent on surface ocean dynamics
983 that influence the degree of nitrate consumption and associated isotope fractionation. Here, we describe local
984 marine N cycling dynamics in order to evaluate whether coral-bound $\delta^{15}\text{N}$ recorded in the *B. elegans* specimens
985 reflects local surface ocean processes.

986 Given complete assimilation of inorganic N pools, the $\delta^{15}\text{N}$ of phytoplankton material - the dominant
987 component of SPOM at the surface ocean - converges on the $\delta^{15}\text{N}$ of the N sources, new nitrate and recycled N
988 sources (Treibergs et al., 2014; Fawcett et al. 2011). At steady state, the $\delta^{15}\text{N}$ of the sinking PON flux reflects the
989 isotope signature of the nitrate upwelled to the surface (Altabet, 1988). Alternatively, given partial nitrate
990 consumption in the context of a finite pool (Rayleigh dynamic), such as in high-nutrient low-chlorophyll regions
991 and in upwelling systems, the SPOM $\delta^{15}\text{N}$ is fractionated relative to the nitrate $\delta^{15}\text{N}$ as function of the
992 assimilation isotope effect and the extent of nitrate consumption (Sigman et al., 1999). The $\delta^{15}\text{N}$ of the sinking
993 flux then reflects both the $\delta^{15}\text{N}$ of nitrate upwelled to the surface and the degree of nitrate consumption (Altabet

Deleted: possible

Deleted: primary

Deleted: ies may differ among asymbiotic coral species and that CWCs may obtain nutrients from a wide range of sources when necessary. For instance, N and C isotope ratios among gorgonian soft coral species collected off the coast of Newfoundland suggest that some feed predominantly on fresh phytodetritus, while others rely on microplankton and thus display higher trophic levels (Sherwood et al., 2008). Additionally, some asymbiotic corals may produce mucus nets to capture suspended particles, whereby corals disperse mucus filaments with their mouth and tentacles and the particles entrapped by the mucus are then drawn back into the mouth for feeding (Lewis and Price, 1975). We observed mucus production by *B. elegans* only when polyps were out of water – a behavior ascribed to the mitigation of dessication (Brown and Bythell, 2005). measurementsthe potential assimilation of wasmarine , (Bronk et al. 2002) (Knapp et al. 2018),...generally
The assertion that metazoan zooplankton are the dominant dietary component of scleractinian CWCs – despite their ability to be omnivorous – is indeed supported by a number of independent studies. The single trophic level between the $\delta^{15}\text{N}$ of zooplankton prey and the soft tissue of many asymbiotic corals has generally been interpreted to indicate that zooplankton are the dominant component of their diet (Duineveld et al., 2004; Sherwood et al. 2005; 2008; 2009; Carlier et al., 2009; Hill et al., 2014; Maier et al., 2020). Additional evidence from lipid biomarkers corroborates the assertion that deep-dwelling CWC species such *Lophelia pertusa* and *Madrepora oculata* feed predominantly on metazoan zooplankton (Dodds et al., 2009; Kiriakoulakis et al., 2005; Naumann et al. 2015). Deep-dwelling CWCs (*Desmophyllum pertusum*, *Madrepora oculata*, *Dendrophyllia cornigera*) also exhibit prey preference for larger zooplankton (Da Ros et al. 2022), suggesting that zooplankton prey are an essential component of their diet. Indeed, an exclusive diet of phytodetritus did not satisfy the fatty acid requirements of *Lophelia pertusa*, requiring supplementation with metazoan zooplankton to achieve maximum growth (Maier et al., 2019). Similarly, zooplankton exclusion from the diet of the solitary CWC *D. dianthus* resulted in a decrease in coral respiration (Naumann et al. 2011). More fundamentally, the shared traits of tentacles and nematocysts are evidence of a predatory life strategy, indicating that zooplankton are an important food source for corals (Lewis and Price, 1975; Sebens et al., 1996). The coral morphology of *B. elegans* and that of other cold water scleractinian corals is consistent with an adaptation for the capture of prey of a commensurate size (Fautin, 2009). Correspondingly, *D. dianthus* is considered to be a generalized zooplankton predator that can prey on medium to large copepods and euphysiids (Höf (... [18])

Formatted: Font color: Text 1

Deleted: faithfulness

Deleted: its

Deleted: to

Formatted: No underline, Font color: Text 1

Formatted: Font: Italic, No underline, Font color: Text 1

Formatted: No underline, Font color: Text 1

Formatted: Font color: Text 1

Deleted: HNLC

1115 and François 1994; François et al. 1997). In this section, we discuss whether coral-bound $\delta^{15}\text{N}$ reflects the $\delta^{15}\text{N}$ of
1116 nitrate entrained to the surface.

1117 Nitrate assimilation at Friday Harbor appeared to be incomplete, potentially implicating the fractionation of
1118 N isotopes between nitrate and biomass. Although depleted nitrate concentrations are generally expected at
1119 coastal sites during the summer in density stratified water column due to phytoplankton assimilation, nitrate
1120 concentrations at Friday Harbor in August of 2021 were upwards of 15 μM at the surface and 20 μM at 30 m
1121 depth. Indeed, nitrate in the San Juan Channel is replete year-round, even at the surface, due to vigorous mixing
1122 within the channel (Mackas and Harrison, 1997; Murray et al., 2015).

1123 The region experiences tidal mixing, designating it as a well-mixed estuary with minimal density
1124 stratification (Banas et al., 1999; Mackas and Harrison, 1997). The tidal influence is clearly identified from the
1125 diurnal patterns of vertical hydrographic structure variability with the salinity/temperature gradients changing
1126 with the tidal phase (Figure 6a and b). The tidal pumping drives vertical mixing between high nutrient deep water
1127 from the Juan de Fuca Strait and fresher surface water from the Strait of Georgia (Banas et al., 1999; Lewis,
1128 1978; Murray et al., 2015; Mackas and Harrison, 1997). Nutrient concentrations in the surface Georgia Strait vary
1129 seasonally and are depleted during the summer at the stratified, fresher surface (Del Bel Belluz et al., 2021;
1130 Mackas and Harrison, 1997). Our temperature-salinity plot in August 2021 reflects end-member mixing between
1131 more saline/colder water from the Juan de Fuca Strait with fresher/warmer surface water from the Georgia Strait
1132 (Figure S9; Banas et al., 1999). The influence of Georgia Strait surface water is recognized by the salinity
1133 minima originating from the outflow of the Fraser River (Figures S10; Mackas and Harrison, 1997). The nitrate
1134 profiles in August 2021, though collected with a lower vertical resolution, do show diurnal variability in vertical
1135 gradients similar to salinity/temperature, consistent with the tidal mixing effect (Figure 6c).

1136 The $\delta^{15}\text{N}$ of nitrate measured at stations near Friday Harbor also corroborate the mixing of nitrate-rich deeper
1137 water with nitrate-deplete surface water from Georgia Strait. The apparent isotope effect for nitrate assimilation
1138 in August 2021 was $\sim 1.5\%$, markedly lower than the canonical value of 5% associated with nitrate assimilation
1139 by surface ocean phytoplankton communities (DiFiore et al., 2006; Sigman et al., 1999; Altabet and François,
1140 1994). A low apparent isotope effect is consistent with two end-member mixing of lower $\delta^{15}\text{N}$, nitrate-rich water
1141 with highly fractionated (high $\delta^{15}\text{N}$), low-nitrate water (Sigman et al., 1999). Highly fractionated nitrate, in turn,
1142 likely originated from nutrient-depleted Georgia Strait surface waters entrained into the Channel Islands. The
1143 linear relationship between salinity and nitrate concentration in August 2021 further substantiates physical
1144 mixing as the dominant control on nitrate concentrations and isotope ratios in San Juan Channel (Figure S10;

Deleted:

Deleted: was ostensibly

Deleted: low surface

Formatted: Font color: Text 1

Deleted: Juan de Fuca Strait as

Deleted: vertical density

Formatted: Font color: Text 1

Deleted: gradients

Deleted: Nutrients are supplied to the broader region by upwelling (Lewis, 1978; Murray et al., 2015; Mackas and Harrison, 1997).

Deleted: The water in the San Juanthis region Channel comprises a mix of ...

Deleted: .

Deleted: , in turn,

Deleted: The

Deleted: s

Deleted: (Figure 6a,b)

Deleted: corroborate

Deleted: of

Formatted: Font color: Text 1

Deleted: and

Deleted: and

Formatted: Font color: Text 1

Formatted: Font color: Text 1

Formatted: Font color: Text 1

Formatted: Font color: Text 1

Deleted: (assimilated)

Formatted: Font color: Text 1

Formatted: Font color: Text 1

Deleted: corroborates

1166 Mackas and Harrison, 1997). Moreover, the $\delta^{15}\text{N}$ of nitrate was relatively uniform with depth, indicating effective
1167 vertical mixing of the Georgia Strait and Juan de Fuca Strait water masses. The relatively slight decrease in
1168 nitrate $\delta^{15}\text{N}$ with depth suggests a secondary influence of local nitrate assimilation on its concentration and
1169 isotope ratios.

1170 The corresponding $\delta^{15}\text{N}$ of SPOM at Friday Harbor covered a broad range, from 4.2 ‰ to 8.7 ‰ in August
1171 2021. The depth distribution of SPOM did not mirror the corresponding nitrate $\delta^{15}\text{N}$ profile, as could otherwise
1172 be expected. At the stratified near-surface (5 m) at station 1, the $\delta^{15}\text{N}$ of SPOM averaged 4.2 ‰ compared to 7.4
1173 ‰ for nitrate. In the context of Rayleigh fractionation, this result suggests that particulate material at the surface
1174 consisted primarily of the instantaneous product of nitrate assimilation (Mariotti et al., 1981). The lower $\delta^{15}\text{N}$
1175 SPOM values could also reflect some degree of reliance on regenerated N species, which would result in $\delta^{15}\text{N}$ of
1176 SPOM lower than that of incident nitrate (Fawcett et al., 2011; Lourey et al., 2003; Treibergs et al., 2014).
1177 Deeper in the water column, the $\delta^{15}\text{N}$ of SPOM converged on the $\delta^{15}\text{N}$ of incident nitrate, between 6 and 7‰,
1178 suggesting that SPOM derived from the complete consumption of an incident nitrate pool (even though nitrate
1179 was present at these depths). Phytoplankton at these depths may thus have originated from surface water
1180 entrained from the Strait of Georgia – where nitrate was completely utilized. The above dynamics complicate
1181 validation of the offset between $\delta^{15}\text{N}$ of exported PON and coral-bound $\delta^{15}\text{N}$. Yet we find little evidence for
1182 nitrate fractionation from partial assimilation on $\delta^{15}\text{N}$ of phytoplankton SPOM, which suggests that the $\delta^{15}\text{N}$
1183 imparted on local *B. elegans* skeletons should reflect the $\delta^{15}\text{N}$ of nitrate entrained to the surface. The ~7‰
1184 difference between coral skeleton $\delta^{15}\text{N}$ (~13.5‰) and the entrained nitrate (~6.5‰) is similar to the empirical
1185 range of 7 - 9‰ reported for other CWC species, (e.g. *D. petusa*, Kiriakoulakis et al., 2005) and *D. dianthus*,
1186 (Wang et al. 2014), and suggests that *B. elegans* provides a record of the thermocline nitrate $\delta^{15}\text{N}$ and surface
1187 nutrient dynamics at Friday Harbor.

1188 5. Conclusions and implications for paleo-reconstruction from coral $\delta^{15}\text{N}$

1189 We conclude that the solitary scleractinian cold water coral *B. elegans* in Friday Harbor, WA predominantly
1190 derives nutrition from metazoan zooplankton prey. While our study was limited to a shallow field site, our
1191 isotope feeding experiment, evaluated alongside previously published studies, points to the possibility that
1192 deeper-dwelling CWCs could also rely on zooplankton prey as a fundamental component of their diet, SPOM
1193 may contribute to these CWCs' diet, but it cannot be presumed to exclusively account for the large offset
1194 between $\delta^{15}\text{N}$ of PON export and coral skeleton $\delta^{15}\text{N}$ documented by Wang et al. (2014). The $\delta^{15}\text{N}$ of skeletal

Formatted: Line spacing: 1.5 lines

Deleted: ...result suggesting...that particulate material at the surface consisted primarily of the instantaneous product of nitrate assimilation (Mariotti et al., 1981). The lower $\delta^{15}\text{N}$ SPOM values could also reflect some degree of reliance on regenerated N species, whose ...hich would result in $\delta^{15}\text{N}$ is ...f SPOM generally (... [19])

Formatted: Font color: Text 1

Deleted: The ...he above dynamics complicate validation of the offset between $\delta^{15}\text{N}$ nitrate (... [20])

Formatted (... [21])

Deleted: . Nevertheless, the offset between nitrate $\delta^{15}\text{N}$ and coral skeleton $\delta^{15}\text{N}$ was on the order of ~6.5 ‰, ...imilar to the empirical range of 7 - 9‰ observed (... [22])

Deleted: *Lophelia* p.;

Deleted: (

Formatted: Font color: Text 1

Formatted (... [23])

Deleted: , suggesting that the $\delta^{15}\text{N}$ imparted on local *B. elegans* skeletons reflects the $\delta^{15}\text{N}$ of nitrate entrained to the surface,

Deleted: . The 1.5 - 2 ‰ difference between the 7‰ offset reported here and that by Wang et al. (8-9‰) might stem from either natural variability between CWC species or the effect of coral habitat depth on the magnitude of the offset. Most of the specimens used in Wang et al. calibration study were collected between ~500 and 1500 m depth and these authors found a small, 1-2‰, increase in the offset magnitude with the depth of coral growth, relatively unaltered by surface nitrate fractionation from partial assim (... [24])

Deleted: may be able to

Deleted: ...urface nutrient dynamics ocean processes (... [25])

Deleted: .

Formatted (... [26])

Deleted: in Friday Harbor, WA

Deleted: shallower-dwelling organisms

Formatted: Font color: Text 1

Formatted: Font color: Text 1

Deleted: a review of related

Formatted: Font color: Text 1

Deleted: studies corroborates that while

Deleted: may

Deleted: be able to feed on a variety of substrates, other s (... [27])

Deleted: , even at abyssal depths

Formatted: Font color: Text 1

Formatted: Font color: Text 1

Formatted: Font color: Text 1

Deleted: intrinsically ...xclusively account for the large o (... [28])

1291 material recovered from coral archives is thus likely to be sensitive to local food web dynamics; for a given $\delta^{15}\text{N}$
 1292 of sinking PON exiting the surface ocean, the $\delta^{15}\text{N}$ recorded by CWC may differ among individuals of the same
 1293 species feeding on different zooplankton prey, depending on availability. In fact, Wang et al. (2014) did report a
 1294 “natural variability” of 1-1.5‰ within a single specimen that might have resulted from some variability of the
 1295 local food web on a short time scale of few years. Some studies have documented an increase in the degree of
 1296 carnivory of zooplankton with depth (Dodds et al., 2009; Vinogradov, 1962). For instance, Hannides et al. (2013)
 1297 recorded a 3.5 ‰ increase in zooplankton $\delta^{15}\text{N}$ from 150 m to 1000 m in the Subtropical North Pacific, with the
 1298 steepest rate of increase from 100 – 300 m. Koppelman et al. (2009) reported a similar pattern of
 1299 zooplankton $\delta^{15}\text{N}$ through the water column. These findings could explain previous reports of small but
 1300 resolvable (1-2 ‰) depth-dependencies of coral $\delta^{15}\text{N}$ (Wang et al. 2014) if corals feed predominantly on
 1301 zooplankton with depth-dependent degree of carnivory of zooplankton and increasing with depth $\delta^{15}\text{N}$. The $\delta^{15}\text{N}$
 1302 recorded in CWC skeletons also tends to differ among species by 1-2‰, as respective species occupy different
 1303 nutritional niches (Tece et al., 2011). The relationship between CWC species represented in fossil archives to
 1304 the depth structure of their zooplankton prey warrants further investigation.

1305 Consideration of the possible dependence of coral-bound $\delta^{15}\text{N}$ on food web dynamics informs the questions
 1306 that can be competently addressed by this proxy. Although we do not have direct estimates of the $\delta^{15}\text{N}$ range that
 1307 can be expected from local food web variability, the scatter around the global compilation of Wang et al. (2014)
 1308 for coral-bound $\delta^{15}\text{N}$ of *D. dianthus* relative to the $\delta^{15}\text{N}$ of PON suggests that this range is modest, on the order of
 1309 ~1-2 ‰. Given this range, we suggest that the coral-bound $\delta^{15}\text{N}$ proxy will be most useful for reconstructing
 1310 larger environmental $\delta^{15}\text{N}$ signals and where chosen coral samples belong to the same species and are collected at
 1311 comparable depths as has already been successfully demonstrated by Wang et al. (2017), Studer et al. (2018) and
 1312 Chen et al. (2023). If used in this way, the broad geographic and temporal coverage afforded by CWCs, the
 1313 opportunity to measure multiple proxies from individual specimens and the imperviousness of coral-bound $\delta^{15}\text{N}$
 1314 to diagenetic alteration render it a valuable paleo-proxy for reconstructing marine N cycling.

1316 **Data Availability** Data presented in this paper is available at: <https://www.bco-dmo.org/project/893811>

1318 **Author Contribution** JG, AG, and MP conceptualized the research presented in this paper. JM and AG designed
 1319 and carried out culture experiments. MP and AC prepared coral samples for analysis. JM and VR analyzed
 1320 samples. JM, AG, JG and KD collected water samples, SPOM, and net tows. KD collected live corals for culture
 1321 experiments and field studies. JM and JG prepared the manuscript with contributions from all co-authors.

Deleted: food ...availability. In fact, Wang et al. (2014) did report a “natural variability” of 1-1.5‰ within a single specimen that might have resulted from some variability of the local food web on a short time scale of few years. Additionally, s (... [29])

Deleted: In this regard, the depth at which corals reside may be an important determinant of their trophic level, due to a...documented an increase in the degree of carnivory of zooplankton with depth (Dodds et al., 2009; Vinogradov, 1962)... For instance, Hannides et al. (2013) recorded a 3.5 ‰ increase in zooplankton $\delta^{15}\text{N}$ from 150 m to 1000 m in the Subtropical North Pacific, with the steepest rate of increase from 100 – 300 m. Koppelman et al. (2009) reported a similar pattern of zooplankton $\delta^{15}\text{N}$ (... [30])

Deleted: studies

Deleted: suggest...ould explain that (... [31])

Formatted: Font color: Text 1

Formatted: Font color: Text 1

Deleted: y

Deleted: could also vary with depth...if they are feeding...predominantly on zooplankton with depth-dependent degree of carnivory of zooplankton and increasing with depth $\delta^{15}\text{N}$. (Wang et al. 2014). ...he $\delta^{15}\text{N}$ recorded in CWC skeletons is (... [32])

Formatted: Font color: Text 1

Formatted: Font color: Text 1

Deleted: We note that t

Deleted: sensitivity ...ossible dependence of the (... [33])

Deleted: to

Deleted: adroitly ...ompetently addressed with ...y thise...proxy.. and the relationship of CWC species represented in fossil archives to the depth structure of zooplankton prey warrants further investigation. ...lthough we do not have direct estimates of the $\delta^{15}\text{N}$ range that can be expected from local food web variability, the scatter around the global compilation of Wang et al. (2014) for coral-bound $\delta^{15}\text{N}$ of *D. dianthus* relative to the $\delta^{15}\text{N}$ of PON suggests that this range is modest, on the order of ~1-2 ‰. Given this range, we suggest that the coral-bound $\delta^{15}\text{N}$ proxy is most useful in systems...ill be most useful for reconstructing larger (... [34])

Deleted: come from

Deleted: correspond

Formatted (... [35])

Deleted: (e.g.,

Deleted: ;

Formatted (... [36])

Formatted: Font color: Text 1

Formatted: Font color: Text 1

Formatted: Indent: First line: 0", Line spacing: 1.5 lines

Deleted: ¶ (... [37])

Formatted: Font color: Text 1

Formatted: Font color: Text 1

1434
1435 **Competing Interests:** The authors declare that they have no conflict of interest.

1436
1437 **Acknowledgements**

1438 We are grateful to Friday Harbor Labs for their assistance with coral collections and field sampling, especially
1439 Pema Kitaeff and Megan Dethier. We acknowledge the valued assistance of the Artemia Reference Center
1440 (specifically Gilbert Van Stappen and Christ Mahieu). Coral culture experiments would not have been sustained
1441 without the help of St. Olaf undergraduate students Rachel Raser, Joash Daniel, Qiantian Nong, YiWynn
1442 Chan, Mansha Haque, [Natasia Preys](#) and Miranda Lenz. We are also indebted to Dr. C. Tobias and P. Ruffino for
1443 access to and assistance with the Elemental Analyzer Isotope Ratio Mass Spectrometer. This project was
1444 funded by an NSF RUI award to A.G. (OCE-1949984), M.G.P (OCE-1949132) and J.G. (OCE-1949119).

1445
1446 **References**

1447 Adams, T.S., Sterner, R.W. 2000. The effect of dietary nitrogen content on trophic level ¹⁵N enrichment. *Limnol.*
1448 *Oceanogr.* 45, 601–607. <https://doi.org/10.4319/lo.2000.45.3.0601>

1449 Adkins, J.F., Henderson, G.M., Wang, S.-L., O’Shea, S., Mokadem, F. 2004. Growth rates of the deep-sea
1450 Scleractinia *Desmophyllum cristagalli* and *Enallopsammia rostrata*. *Earth and Planetary Science Letters*
1451 227, 481–490. <https://doi.org/10.1016/j.epsl.2004.08.022>

1452 Al-Moghrabi, S., Allemand, D. & Jaubert, J. 1993. Valine uptake by the scleractinian coral *Galaxea fascicularis*:
1453 characterization and effect of light and nutritional status. *J Comp Physiol B* 163, 355–362.
1454 <https://doi.org/10.1007/BF00265638>

1455 Altabet, M.A., 1988. Variations in nitrogen isotopic composition between sinking and suspended particles:
1456 implications for nitrogen cycling and particle transformation in the open ocean. *Deep Sea Res. Part*
1457 *Oceanogr. Res. Pap.* 35, 535–554. [https://doi.org/10.1016/0198-0149\(88\)90130-6](https://doi.org/10.1016/0198-0149(88)90130-6)

1458 Altabet, M.A., Deuser, W.G., Honjo, S., Stienen, C., 1991. Seasonal and depth-related changes in the source of
1459 sinking particles in the North Atlantic. *Nature* 354, 136–139. <https://doi.org/10.1038/354136a0>

1460 Altabet, M.A., Francois, R., 1994. Sedimentary nitrogen isotopic ratio as a recorder for surface ocean nitrate
1461 utilization. *Glob. Biogeochem. Cycles* 8, 103–116. <https://doi.org/10.1029/93GB03396>

1462 Altabet, M., Higgins, M. & Murray, D. 2002. The effect of millennial-scale changes in Arabian Sea
1463 denitrification on atmospheric CO₂. *Nature* 415, 159–162. <https://doi.org/10.1038/415159a>

1464 Ayliffe, L.K., Cerling, T.E., Robinson, T., West, A.G., Sponheimer, M., Passey, B.H., Hammer, J., Roeder, B.,
1465 Dearing, M.D., Ehleringer, J.R., 2004. Turnover of carbon isotopes in tail hair and breath CO₂ of horses
1466 fed an isotopically varied diet. *Oecologia* 139, 11–22. <https://doi.org/10.1007/s00442-003-1479-x>

1467 Banas, N., Bricker, J., Carter, G., Gerdes, F., Martin, W., Nelson, E., Ross, T., Scansen, B., Simons, R., Wells,
1468 M., 1999. Flow, Stratification, and mixing in San Juan Channel.

1469 [Beauchamp, K.A., 1989. Aspects of gametogenesis, development and planulation in laboratory populations of](#)
1470 [solitary corals and corallimorpharian sea anemones \(Ph.D.\). University of California, Santa Cruz, United](#)
1471 [States -- California.](#)

Deleted: u

Formatted: Font color: Text 1

Formatted: Font color: Text 1

Formatted: Font color: Text 1

Formatted: Font color: Text 1

Formatted: Font color: Text 1

Deleted: Alldredge, A.L., King, J.M., 1977. Distribution, abundance, and substrate preferences of demersal reef zooplankton at Lizard Island Lagoon, Great Barrier Reef. *Mar. Biol.* 41, 317–333. <https://doi.org/10.1007/BF00389098>

Formatted: Font color: Text 1

Formatted: Font color: Text 1

Formatted: Font color: Text 1

Formatted: Font color: Text 1

Formatted: Font color: Text 1

Formatted: Font color: Text 1

Formatted: Font: 11 pt, Font color: Text 1

Formatted: Normal, Indent: Left: 0", Hanging: 0.5", Space Before: 0 pt, After: 0 pt

Formatted: Font color: Text 1

1477 Böhlke, J.K., Mroczkowski, S.J., Coplen, T.B., 2003. Oxygen isotopes in nitrate: new reference materials for
1478 18O:17O:16O measurements and observations on nitrate-water equilibration. *Rapid Commun. Mass*
1479 *Spectrom.* RCM 17, 1835–1846. <https://doi.org/10.1002/rcm.1123>

1480 Braman, R.S., Hendrix, S.A., 1989. Nanogram nitrite and nitrate determination in environmental and biological
1481 materials by vanadium(III) reduction with chemiluminescence detection. *Anal. Chem.* 61, 2715–2718.
1482 <https://doi.org/10.1021/ac00199a007>

1483 Brandes, J.A., Devol, A.H., 2002. A global marine-fixed nitrogen isotopic budget: Implications for Holocene
1484 nitrogen cycling. *Glob. Biogeochem. Cycles* 16, 67-1-67–14. <https://doi.org/10.1029/2001GB001856>

1485 Brnk, D. A. 2002. Dynamics of DON. *Biogeochem. Mar. Dissolved Org. Matter* 153–249.

1486 Brown, B. E., & Bythell, J. C. 2005. Perspectives on mucus secretion in reef corals. *Marine Ecology Progress*
1487 *Series*, 296, 291–309. <http://www.jstor.org/stable/24868640>Cairns, S.D., 2007. Deep-water corals: an
1488 overview with special reference to diversity and distribution of deep-water scleractinian corals. *Bull.*
1489 *Mar. Sci.* 81, 311–322.

1490 Carlier, A., Guilloux, E.L., Olu, K., Sarrazin, J., Mastrototaro, F., Taviani, M., Clavier, J., 2009. Trophic
1491 relationships in a deep Mediterranean cold-water coral bank (Santa Maria di Leuca, Ionian Sea). *Mar.*
1492 *Ecol. Prog. Ser.* 397, 125–137. <https://doi.org/10.3354/meps08361>

1493 Carpenter, E. J., Harvey, H. R., Fry, B. & Capone, D. G. 1997. Biogeochemical tracers of the marine
1494 cyanobacterium *Trichodesmium*. *Deep-Sea Res. I* 44, 27–38. [doi.org/10.1016/S0967-0637\(96\)00091-X](https://doi.org/10.1016/S0967-0637(96)00091-X)

1495 Casciotti, K.L., Sigman, D.M., Hastings, M.G., Böhlke, J.K., Hilkert, A., 2002. Measurement of the oxygen
1496 isotopic composition of nitrate in seawater and freshwater using the denitrifier method. *Anal. Chem.* 74,
1497 4905–4912. <https://doi.org/10.1021/ac020113w>

1498 Casciotti, K.L., Trull, T.W., Glover, D.M., Davies, D., 2008. Constraints on nitrogen cycling at the subtropical
1499 North Pacific Station ALOHA from isotopic measurements of nitrate and particulate nitrogen. *Deep Sea*
1500 *Res. Part II Top. Stud. Oceanogr.* 55, 1661–1672. <https://doi.org/10.1016/j.dsr2.2008.04.017>

1501 Cathalot C, Van Oevelen D, Cox TJS, Kutti T, Lavaley M., Duineveld G., Meysman F. J. R. 2015. Cold-water
1502 coral reefs and adjacent sponge grounds: hotspots of benthic respiration and organic carbon cycling in the
1503 deep sea. *Front Mar Sci* 2. <https://www.frontiersin.org/articles/10.3389/fmars.2015.00037>.

1504 Cerling, T.E., Ayliffe, L.K., Dearing, M.D., Ehleringer, J.R., Passey, B.H., Podlesak, D.W., Torregrossa, A-M.,
1505 West, A.G. 2007. Determining biological tissue turnover using stable isotopes: the reaction progress
1506 variable. *Ecophysiology* 151, 175-189. <https://doi.org/10.1007/s00442-006-0571-4>

1507 Chen, WH., Ren, H., Chiang, J.C.H. *et al.* Increased tropical South Pacific western boundary current transport
1508 over the past century. *Nat. Geosci.* 16, 590–596 (2023). <https://doi.org/10.1038/s41561-023-01212-4>

1509 Cheng, H., Adkins, J., Edwards, R.L., Boyle, E.A., 2000. U-Th dating of deep-sea corals. *Geochim. Cosmochim.*
1510 *Acta* 64, 2401–2416. [https://doi.org/10.1016/S0016-7037\(99\)00422-6](https://doi.org/10.1016/S0016-7037(99)00422-6)

1511 Crook, E.D., Cooper, H., Potts, D.C., Lambert, T., Paytan, A., 2013. Impacts of food availability and pCO₂ on
1512 planulation, juvenile survival, and calcification of the azooxanthellate scleractinian coral *Balanophyllia*
1513 *elegans*. *Biogeosciences* 10, 7599–7608. <https://doi.org/10.5194/bg-10-7599-2013>

1514 Da Ros, Z., Dell’Anno, A., Fanelli, E., Angeletti, L., Taviani, M., Danovaro, R., 2022. Food preferences of
1515 Mediterranean cold-water corals in captivity. *Front. Mar. Sci.* 9.

Formatted: Font color: Text 1

Formatted: Font color: Text 1

Formatted: No underline, Font color: Text 1

Formatted: Font: 11 pt, Font color: Text 1

Formatted: No underline, Font color: Text 1

Formatted: Default Paragraph Font, Font: 11 pt, Font color: Text 1

Formatted: Font color: Text 1

Formatted: Normal, Space Before: 0 pt, After: 0 pt

Formatted: Font color: Text 1

Formatted: Font color: Text 1

Formatted: Font color: Text 1

Formatted: Font color: Text 1

Formatted: Font color: Text 1

Formatted: Font color: Text 1

Formatted: Font color: Text 1

Formatted: Font color: Text 1

Deleted: Cohen, A.L., Gaetani, G.A., Lundqvist, T., Cortiss, B.H., George, R.Y., 2006. Compositional variability in a cold-water scleractinian, *Lophelia pertusa*: New insights into “vital effects.” *Geochem. Geophys. Geosystems* 7. <https://doi.org/10.1029/2006GC001354>
Corbera, G., Lo Iacono, C., Simarro, G. *et al.* 2022. Local-scale feedbacks influencing cold-water coral growth and subsequent reef formation. *Sci Rep* 12, 20389. <https://doi.org/10.1038/s41598-022-24711-7>

Formatted: Font color: Text 1

- 1525 Del Bel Belluz, J., Peña, M.A., Jackson, J.M., Nemcek, N., 2021. Phytoplankton composition and environmental
 1526 drivers in the Northern Strait of Georgia (Salish Sea), British Columbia, Canada. *Estuaries Coasts* 44,
 1527 1419–1439. <https://doi.org/10.1007/s12237-020-00858-2>.
- 1528 De Pol-Holz R, Robinson RS, Hebbeln D, Sigman DM, Ulloa O. 2009. Controls on sedimentary nitrogen
 1529 isotopes along the Chile margin. *Deep Res Part II Top Stud Oceanogr* 56(16).
 1530 doi:10.1016/j.dsr2.2008.09.014
- 1531 DiFiore, P.J., Sigman, D.M., Trull, T.W., Lourey, M.J., Karsh, K., Cane, G., Ho, R., 2006. Nitrogen isotope
 1532 constraints on subantarctic biogeochemistry. *J. Geophys. Res. Oceans* 111.
 1533 <https://doi.org/10.1029/2005JC003216>
- 1534 Dodds, L.A., Black, K.D., Orr, H., Roberts, J.M., 2009. Lipid biomarkers reveal geographical differences in food
 1535 supply to the cold-water coral *Lophelia pertusa* (Scleractinia). *Mar. Ecol. Prog. Ser.* 397, 113–124.
 1536 <https://doi.org/10.3354/meps08143>
- 1537 Doi, H., Akamatsu, F., González, A.L., 2017. Starvation effects on nitrogen and carbon stable isotopes of
 1538 animals: an insight from meta-analysis of fasting experiments. *R. Soc. Open Sci.* 4, 170633.
 1539 <https://doi.org/10.1098/rsos.170633>
- 1540 Drake, J.L., Guillermic, M., Eagle, R.A., Jacobs, D.K., 2021. Fossil corals with various degrees of preservation
 1541 can retain information about biomineralization-related organic material. *Front. Earth Sci.* 9.
- 1542 Druffel, E.R.M., 1997. Geochemistry of corals: Proxies of past ocean chemistry, ocean circulation, and climate.
 1543 *Proc. Natl. Acad. Sci.* 94, 8354–8361. <https://doi.org/10.1073/pnas.94.16.8354>.
- 1544 Duineveld, G.C.A., Lavaleye, M.S.S., Berghuis, E.M., 2004. Particle flux and food supply to a seamount cold-
 1545 water coral community (Galicia Bank, NW Spain). *Mar. Ecol. Prog. Ser.* 277, 13–23.
 1546 <https://doi.org/10.3354/meps277013>
- 1547 Duineveld, G., Lavaleye, M., Bergman, M., Stigter, H., Mienis, F., 2007. Trophic structure of a cold-water coral
 1548 mound community (Rockall Bank, NE Atlantic) in relation to the near-bottom particle supply and current
 1549 regime. *Bull. Mar. Sci.* 81, 449–467.
- 1550 ~~Durham, J. W., and Barnard, J.L., 1952. Stony corals of the Eastern Pacific collected by the Velero III and Velero
 1551 IV. All an Hancock Pacific Expeditions 16, 1-110.~~
- 1552 Erler, D.V., Wang, X.T., Sigman, D.M., Scheffers, S.R., Shepherd, B.O., 2015. Controls on the nitrogen isotopic
 1553 composition of shallow water corals across a tropical reef flat transect. *Coral Reefs* 34, 329–338.
 1554 <https://doi.org/10.1007/s00338-014-1215-5>.
- 1555 Esri. "Ocean" [basemap]. Scale Not Given. "Ocean Basemap". February 11, 2021.
 1556 [https://hub.arcgis.com/maps/CESPK::ocean-basemap/explore?location=35.956244%2C-](https://hub.arcgis.com/maps/CESPK::ocean-basemap/explore?location=35.956244%2C-111.078800%2C5.00)
 1557 [111.078800%2C5.00](https://hub.arcgis.com/maps/CESPK::ocean-basemap/explore?location=35.956244%2C-111.078800%2C5.00). (December, 2022).
- 1558 Fadlallah, Y.H., 1983. Population Dynamics and Life History of a Solitary Coral, *Balanophyllia elegans*, from
 1559 Central California. *Oecologia* 58, 200–207.
- 1560 Fautin, D.G., 2009. Structural diversity, systematics, and evolution of cnidae. *Toxicon, Cnidarian Toxins and*
 1561 *Venoms* 54, 1054–1064. <https://doi.org/10.1016/j.toxicon.2009.02.024>

Formatted: Font color: Text 1

Formatted: Font color: Text 1

Formatted: Font color: Text 1

Formatted: Font color: Text 1

Formatted: Font color: Text 1

Formatted: Font color: Text 1

Formatted: Font: 11 pt, Font color: Text 1

Formatted: Font color: Text 1

~~Deleted: Duineveld GCA, Jeffreys RM, Lavaleye MSS, Davies AJ, Bergman MN, Watmough T, Witbaard R. 2012. Spatial and tidal variation in food supply to shallow cold-water coral reefs of the Mingulay Reef complex (Outer Hebrides, Scotland). *Mar Ecol Prog Ser* 444:97-115. <https://doi.org/10.3354/meps09428>~~

Formatted: Font color: Text 1

Formatted: Font color: Text 1

Formatted: Font color: Text 1

- 1567 Fawcett, S.E., Lomas, M.W., Casey, J.R., Ward, B.B., Sigman, D.M., 2011. Assimilation of upwelled nitrate by
1568 small eukaryotes in the Sargasso Sea. *Nat. Geosci.* 4, 717–722. <https://doi.org/10.1038/ngeo1265>
- 1569 Ferrier, M.D. 1991. Net uptake of dissolved free amino acids by four scleractinian corals. *Coral Reefs* 10, 183–
1570 187. <https://doi.org/10.1007/BF00336772>
- 1571 François, R., Altabet, M.A., Yu, E.-F., Sigman, D.M., Bacon, M.P., Frank, M., Bohrmann, G., Bareille, G.,
1572 Labeyrie, L.D., 1997. Contribution of Southern Ocean surface-water stratification to low atmospheric
1573 CO2 concentrations during the last glacial period. *Nature* 389, 929–935. <https://doi.org/10.1038/40073>
- 1574 Freiwald, A. 2002. Reef-Forming Cold-Water Corals. In: Wefer, G., Billett, D., Hebbeln, D., Jørgensen, B.B.,
1575 Schlüter, M., van Weering, T.C.E. (eds) *Ocean Margin Systems*. Springer, Berlin, Heidelberg.
1576 https://doi.org/10.1007/978-3-662-05127-6_23
- 1577 Gagnon, A.C., Gothmann, A.M., Branson, O., Rae, J.W.B., Stewart, J.A., 2021. Controls on boron isotopes in a
1578 cold-water coral and the cost of resilience to ocean acidification. *Earth and Planetary Science Letters*
1579 554, 116662. <https://doi.org/10.1016/j.epsl.2020.116662>
- 1580 Ganeshram, R. S., and Pedersen, T. F. 1998. Glacial-interglacial variability in upwelling and bioproductivity off
1581 NW Mexico: Implications for Quaternary paleoclimate, *Paleoceanography*, 13(6), 634– 645,
1582 doi:10.1029/98PA02508.
- 1583 Garcia-Herrera, N., Cornils, A., Laudien, J., Niehoff, B., Höfer, J., Försterra, G., González, H.E., Richter, C.,
1584 2022. Seasonal and diel variations in the vertical distribution, composition, abundance and biomass of
1585 zooplankton in a deep Chilean Patagonian Fjord. *PeerJ* 10, e12823. <https://doi.org/10.7717/peerj.12823>
- 1586 Genin, A., Dayton, P.K., Lonsdale, P.F., Spiess, F.N., 1986. Corals on seamount peaks provide evidence of
1587 current acceleration over deep-sea topography. *Nature* 322, 59–61. <https://doi.org/10.1038/322059a0>
- 1588 Gerrodette, T. 1981. *Equatorial Submergence in a Solitary Coral, Balanophyllia elegans, and the Critical Life*
1589 *Stage Excluding the Species from Shallow Water in the South*. *Mar. Ecol. Prog. Series* 1, 227-235.
1590 <http://www.jstor.org/stable/24812947>
- 1591 Gonfiantini, R., W. Stichler, and K. Rosanski 1995, Standards and Intercomparison. Materials Distributed by the
1592 IAEA for Stable Isotope Measurements, Int. At. Energy Agency, Vienna.
- 1593 Goodfriend, G.A., Hare, P.E., Druffel, E.R.M. 1992. Aspartic acid racemization and protein diagenesis in corals
1594 over the last 350 years. *Geochim. Cosmochim. Acta* 56, 3847–3850. [https://doi.org/10.1016/0016-7037\(92\)90176-J](https://doi.org/10.1016/0016-7037(92)90176-J)
- 1595
- 1596
- 1597 Gori, A., R. Grover, C. Orejas, S. Sikorski, and C. Ferrier-Pagès. 2014. Uptake of dissolved free amino acids by
1598 four cold-water coral species from the Mediterranean Sea. *Deep Sea Res. Part II Top. Stud. Oceanogr.*
1599 99: 42–50. doi:10.1016/j.dsr2.2013.06.007.
- 1600 Gothmann AM, Stolarski J, Adkins JF, et al. Fossil corals as an archive of secular variations in seawater
1601 chemistry since the Mesozoic. *Geochim Cosmochim Acta*. 2015;160:188-208.
1602 doi:https://doi.org/10.1016/j.gca.2015.03.018
- 1603 Grover, R. Maguer, J-F, Allemand, D., Ferrier-Pagès, C. 2008. Uptake of dissolved free amino acids by the
1604 scleractinian coral *Stylophora pistillata*. *J Exp Biol* 211 (6): 860–865. doi:
1605 <https://doi.org/10.1242/jeb.012807>

Formatted: Font color: Text 1

Formatted: Font color: Text 1

Formatted: Font color: Text 1

Formatted: Font color: Text 1

Formatted: Font color: Text 1

Formatted: Font color: Text 1

Formatted: Font: 11 pt, Font color: Text 1

Formatted: Normal, Indent: Left: 0", Hanging: 0.5", Space Before: 0 pt, After: 0 pt

Deleted: ¶

Formatted: Font color: Text 1

Formatted: Font: 11 pt, Font color: Text 1

Formatted: Font color: Text 1

Formatted: Font: (Default) Times New Roman, Font color: Text 1

Formatted: Font: (Default) Times New Roman, No underline, Font color: Text 1

Formatted: Font: (Default) Times New Roman, 11 pt, Font color: Text 1

Formatted: Font: (Default) Times New Roman, No underline, Font color: Text 1

Formatted: Font: (Default) Times New Roman, 11 pt, Font color: Text 1

Formatted: Bibliography, Space Before: 0.6 line, After: 0.6 line

Formatted: Font: 11 pt, Font color: Text 1

Deleted: ¶

Formatted: Font: (Default) Times New Roman, Font color: Text 1

Formatted: ... [38]

Formatted: Font color: Text 1

Formatted: Font: 11 pt, Font color: Text 1

Formatted: ... [39]

Formatted: Font: 11 pt, No underline, Font color: Text 1

Formatted: ... [40]

Formatted: Space Before: 0 pt, After: 0 pt

Deleted: ¶

Formatted: ... [41]

Formatted: Font color: Text 1

Deleted: Renaud

Formatted: Font: 11 pt, Font color: Text 1

Formatted: Font color: Text 1

- 1610 Hannides, Cecelia C. S., Popp, Brian N., Choy, C. Anela, Drazen, Jeffrey C. 2013. Midwater zooplankton and
 1611 suspended particle dynamics in the North Pacific Subtropical Gyre: A stable isotope perspective,
 1612 *Limnology and Oceanography*, 58, doi: 10.4319/lo.2013.58.6.1931.
- 1613 Hill, T.M., Myrsvold, C.R., Spero, H.J., Guilderson, T.P. 2014. Evidence for benthic and pelagic food web
 1614 coupling and carbon export from California margin bamboo coral archives. *Biogeosciences* 11, 3845–
 1615 3854. <https://doi.org/10.5194/bg-11-3845-2014>.
- 1616 Hines, S.K.V., Southon, J.R., Adkins, J.F. 2015. A high-resolution record of Southern Ocean intermediate water
 1617 radiocarbon over the past 30,000 years. *Earth and Planetary Science Letters* 432, 46–58.
 1618 <https://doi.org/10.1016/j.epsl.2015.09.038>.
- 1619 Hoegh-Guldberg, O., Williamson, J. Availability of two forms of dissolved nitrogen to the coral *Pocillopora*
 1620 *damicornis* and its symbiotic zooxanthellae. *Marine Biology* 133, 561–570 (1999).
 1621 <https://doi.org/10.1007/s002270050496>
- 1622 Höfer, J., González, H.E., Laudien, J., Schmidt, G.M., Häussermann, V., Richter, C., 2018. All you can eat: the
 1623 functional response of the cold-water coral *Desmophyllum dianthus* feeding on krill and copepods. *PeerJ*
 1624 6, e5872. <https://doi.org/10.7717/peerj.5872>
- 1625 Horn, M.G., Robinson, R.S., Rynearson, T.A., Sigman, D.M., 2011. Nitrogen isotopic relationship between
 1626 diatom-bound and bulk organic matter of cultured polar diatoms. *Paleoceanography* 26.
 1627 <https://doi.org/10.1029/2010PA002080>.
- 1628 Kast, E.R., Stolper, D.A., Auderset, A., Higgins, J.A., Ren, H., Wang, X.T., Martínez-García, A., Haug, G.H.,
 1629 Sigman, D.M., 2019. Nitrogen isotope evidence for expanded ocean suboxia in the early Cenozoic.
 1630 *Science* 364, 386–389. <https://doi.org/10.1126/science.aau5784>
- 1631 Kiriakoulakis, K., Fisher, E., Wolff, G.A., Freiwald, A., Grehan, A., Roberts, J.M., 2005. Lipids and nitrogen
 1632 isotopes of two deep-water corals from the North-East Atlantic: initial results and implications for their
 1633 nutrition, in: Freiwald, A., Roberts, J.M. (Eds.), *Cold-Water Corals and Ecosystems*, Erlangen Earth
 1634 Conference Series. Springer, Berlin, Heidelberg, pp. 715–729. https://doi.org/10.1007/3-540-27673-4_37.
- 1635 ~~Knapp, A. N., K. L. Casciotti, and M. G. Prokopenko. 2018. Dissolved Organic Nitrogen Production and~~
 1636 ~~Consumption in Eastern Tropical South Pacific Surface Waters. *Glob. Biogeochem. Cycles* 32: 769–783.~~
 1637 ~~doi:10.1029/2017GB005875~~
- 1638 Knapp AN, DiFiore PJ, Deutsch C, Sigman DM, Lipschultz F. 2008. Nitrate isotopic composition between
 1639 Bermuda and Puerto Rico: Implications for N₂ fixation in the Atlantic Ocean. *Global Biogeochem Cycles*
 1640 22(3). doi:10.1029/2007GB003107
- 1641 Koppelman, R., Böttger-Schnack, R., Möbius, J., Weikert, H., 2009. Trophic relationships of zooplankton in the
 1642 eastern Mediterranean based on stable isotope measurements. *Journal of Plankton Research* 31, 669–686.
- 1643 Lasker, H.R., 1981. A comparison of the particulate feeding abilities of three species of Gorgonian soft coral.
 1644 *Mar. Ecol. Prog. Ser.* 5, 61–67.
- 1645 Lewis, A.G., 1978. Concentrations of nutrients and chlorophyll on a cross-channel transect in Juan de Fuca Strait,
 1646 British Columbia. *J. Fish. Res. Board Can.* 35, 305–314. <https://doi.org/10.1139/f78-055>

Formatted: No underline, Font color: Text 1

Formatted: Font color: Text 1

Formatted: Font: 11 pt, Font color: Text 1

Formatted: No underline, Font color: Text 1

Formatted: Font color: Text 1

Formatted: Font: 11 pt, Font color: Text 1

Formatted: No underline, Font color: Text 1

Formatted: Font color: Text 1

Formatted: Font: 11 pt, Font color: Text 1

Formatted: Font color: Text 1

~~Deleted: Houlbrèque F, Tambutté E, Allemand D, Ferrier-Pagès C. 2004. Interactions between zooplankton feeding, photosynthesis and skeletal growth in the scleractinian coral *Stylophora pistillata*. *J Exp Biol.* 4 Apr;207(Pt 9):1461-9. doi: 10.1242/jeb.009111. PMID: 15037640.~~

Formatted: Font color: Text 1

Formatted: No underline, Font color: Text 1

Formatted: Font: 11 pt, Font color: Text 1

Formatted: No underline, Font color: Text 1

Formatted: Font: 11 pt, Font color: Text 1

Formatted: Bibliography, Space Before: 0.6 line, After: 0.6 line

Deleted: ¶

Deleted: <inf>2</inf>

Formatted: Font color: Text 1

Deleted: ¶

~~Deleted: Kuanui P, Chavanich S, Viyakam V, Omori M, Fujita T, Lin C. 2020. Effect of light intensity on survival and photosynthetic efficiency of cultured corals of different ages. *Estuar Coast Shelf Sci.* 235:106515. doi:https://doi.org/10.1016/j.eess.2019.106515~~
~~Knutson, D.W., Buddemeier, R.W., Smith, S.V., 1972. Coral chronometers: Seasonal growth bands in reef corals. *Science* 177, 270–272. <https://doi.org/10.1126/science.177.4045.270>~~
~~Larsson AI, Lundälv T, van Oevelen D. 2013. Skeletal growth, respiration rate and fatty acid composition in the cold-water coral *Lophelia pertusa* under varying food conditions. *Mar Ecol Prog Ser* 483:169–184. <https://doi.org/10.3354/meps10284>~~

Formatted: Font color: Text 1

1667 Lewis, J.B., Price, W.S., 1975. Feeding mechanisms and feeding strategies of Atlantic reef corals. *J. Zool.* 176,
1668 527–544. <https://doi.org/10.1111/j.1469-7998.1975.tb03219.x>

1669 [Li, T., Robinson, L.F., Chen, T., Wang, X.T., Burke, A., Rae, J.W.B., Pegrum-Haram, A., Knowles, T.D.J., Li,
1670 G., Chen, J., Ng, H.C., Prokopenko, M., Rowland, G.H., Samperiz, A., Stewart, J.A., Southon, J.,
1671 Spooner, P.T., 2020. Rapid shifts in circulation and biogeochemistry of the Southern Ocean during
1672 deglacial carbon cycle events. *Science Advances* 6, eabb3807](#)

1673 ▲

1674 Lourey, M.J., Trull, T.W., Sigman, D.M., 2003. Sensitivity of $\delta^{15}\text{N}$ of nitrate, surface suspended and deep
1675 sinking particulate nitrogen to seasonal nitrate depletion in the Southern Ocean. *Glob. Biogeochem.*
1676 *Cycles* 17. <https://doi.org/10.1029/2002GB001973>

1677 Mackas, D.L., Harrison, P.J., 1997. Nitrogenous nutrient sources and sinks in the Juan de Fuca Strait/Strait of
1678 Georgia/Puget Sound estuarine system: Assessing the potential for eutrophication. *Estuar. Coast. Shelf*
1679 *Sci.* 44, 1–21. <https://doi.org/10.1006/ecss.1996.0110>

1680 Maier, S.R., Bannister, R.J., van Oevelen, D., Kutti, T., 2020. Seasonal controls on the diet, metabolic activity,
1681 tissue reserves and growth of the cold-water coral *Lophelia pertusa*. *Coral Reefs* 39, 173–187.
1682 <https://doi.org/10.1007/s00338-019-01886-6>

1683 [Maier, S.R., Kutti, T., Bannister, R.J., van Breugel, P., van Rijswijk, P., van Oevelen, D., 2019. Survival under
1684 conditions of variable food availability: Resource utilization and storage in the cold-water coral *Lophelia*
1685 *pertusa*. *Limnol. Oceanogr.* 64, 1651–1671. <https://doi.org/10.1002/lno.11142>](#)

1686 [Maier, S.R., Brooke, S., De Clippele, L.H., de Froc, E., van der Kaaden, A.-S., Kutti, T., Mienis, F., van Oevelen,
1687 D., 2023. On the paradox of thriving cold-water coral reefs in the food-limited deep sea. *Biological*
1688 *Reviews* 98, 1768–1795. <https://doi.org/10.1111/brv.12976>](#)

1689 Marconi D, Weigand AM, Rafter PA, Matthew R. McIlvin MR, Matthew Forbes, M Casciotti, KL Sigman, DM.
1690 2015. Nitrate isotope distributions on the US GEOTRACES North Atlantic cross-basin section: Signals of
1691 polar nitrate sources and low latitude nitrogen cycling. *Mar Chem.* 177:143-156.
1692 doi:<https://doi.org/10.1016/j.marchem.2015.06.007>

1693 [Margolin, A. R., L. F. Robinson, A. Burke, R. G. Waller, K. M. Scanlon, M. L. Roberts, M. E. Auro, and T. van
1694 de Fliedrt. 2014. Temporal and spatial distributions of cold-water corals in the Drake Passage: Insights
1695 from the last 35,000 years. *Deep Sea Res. Part II Top. Stud. Oceanogr.* 99: 237–248.
1696 doi:10.1016/j.dsr2.2013.06.008](#)

1697 Mariotti, A., Germon, J.C., Hubert, P., Kaiser, P., Letolle, R., Tardieux, A., Tardieux, P., 1981. Experimental
1698 determination of nitrogen kinetic isotope fractionation: Some principles; illustration for the
1699 denitrification and nitrification processes. *Plant Soil* 62, 413–430. <https://doi.org/10.1007/BF02374138>

1700 Martínez del Río, C., Carleton, S.A., 2012. How fast and how faithful: the dynamics of isotopic incorporation
1701 into animal tissues. *J. Mammal.* 93, 353–359. <https://doi.org/10.1644/11-MAMM-S-165.1>

1702 McCutchan Jr, J.H., Lewis Jr, W.M., Kendall, C., McGrath, C.C., 2003. Variation in trophic shift for stable
1703 isotope ratios of carbon, nitrogen, and sulfur. *Oikos* 102, 378–390. [https://doi.org/10.1034/j.1600-
0706.2003.12098.x](https://doi.org/10.1034/j.1600-
1704 0706.2003.12098.x)

Formatted: Hyperlink, Font color: Text 1

Field Code Changed

Formatted: Font: (Default) +Body (Times New Roman), 11 pt, Font color: Text 1

Formatted: Indent: Left: 0", Hanging: 0.5"

Formatted: Font: +Body (Times New Roman), Font color: Text 1

Formatted: Normal, Space Before: 0 pt, After: 0 pt

Formatted: Font color: Text 1

Formatted: Font: 11 pt, Font color: Text 1

Formatted: Font color: Text 1

~~Deleted: Maier C, Hegeman J, Weinbauer MG, Gattuso J-P. Calcification of the cold-water coral *Lophelia pertusa*, under ambient and reduced pH. *Biogeosciences*. 2009;6(8):1671-1680. doi:10.5194/bg-6-1671-2009~~

Formatted: Font color: Text 1

Formatted: Font: 11 pt, Font color: Text 1

Formatted: No underline

Formatted: Font: 11 pt, Font color: Text 1

Formatted: Font: 11 pt, Font color: Text 1

Formatted: Font color: Text 1

Formatted: Font color: Text 1

Formatted

Formatted: Font color: Text 1

- 1709 McIlvin, M.R., Casciotti, K.L., 2011. Technical Updates to the Bacterial Method for Nitrate Isotopic Analyses.
1710 Anal. Chem. 83, 1850–1856. <https://doi.org/10.1021/ac1028984>
- 1711 McMahon, K.W., Williams, B., Guilderson, T.P., Glynn, D.S., McCarthy, M.D., 2018. Calibrating amino acid
1712 $\delta^{13}\text{C}$ and $\delta^{15}\text{N}$ offsets between polyp and protein skeleton to develop proteinaceous deep-sea corals as
1713 paleoceanographic archives. *Geochim. Cosmochim. Acta* 220, 261–275.
1714 <https://doi.org/10.1016/j.gca.2017.09.048>
- 1715 Middelburg, J., Mueller, C., Veuger, B. Larsson, A. I., Form, A., van Oevelen, D 2016.. Discovery of symbiotic
1716 nitrogen fixation and chemoautotrophy in cold-water corals. *Sci Rep* 5, 17962 (2016).
1717 <https://doi.org/10.1038/srep17962>
- 1718 Miller, M., 1995. Growth of a temperate coral: effects of temperature, light, depth, and heterotrophy. *Mar. Ecol.*
1719 *Prog. Ser.* 122, 217–225. <https://doi.org/10.3354/meps122217>
- 1720 Minagawa, M., Wada, E., 1984. Stepwise enrichment of ^{15}N along food chains: Further evidence and the relation
1721 between $\delta^{15}\text{N}$ and animal age. *Geochim. Cosmochim. Acta* 48, 1135–1140.
1722 [https://doi.org/10.1016/0016-7037\(84\)90204-7](https://doi.org/10.1016/0016-7037(84)90204-7)
- 1723 Mortensen P.B., (2001) Aquarium observations on the deep-water coral *Lophelia pertusa* (L., 1758) (scleractinia)
1724 and selected associated invertebrates, *Ophelia*, 54:2, 83-104, DOI: 10.1080/00785236.2001.10409457
- 1725 Muhs, D.R., Kennedy, G.L., Rockwell, T.K., 1994. Uranium-Series Ages of Marine Terrace Corals from the
1726 Pacific Coast of North America and Implications for Last-Interglacial Sea Level History. *Quaternary*
1727 *Research* 42, 72–87. <https://doi.org/10.1006/qres.1994.1055>
- 1728 Mueller, C.E., Larsson, A.I., Veuger, B., Middelburg, J.J., van Oevelen, D., 2014. Opportunistic feeding on
1729 various organic food sources by the cold-water coral *Lophelia pertusa*. *Biogeosciences* 11, 123–133.
1730 <https://doi.org/10.5194/bg-11-123-2014>
- 1731 Murray, J.W., Roberts, E., Howard, E., O'Donnell, M., Bantam, C., Carrington, E., Foy, M., Paul, B., Fay, A.,
1732 2015. An inland sea high nitrate-low chlorophyll (HNLC) region with naturally high pCO₂. *Limnol.*
1733 *Oceanogr.* 60, 957–966. <https://doi.org/10.1002/lno.10062>
- 1734 Muscatine, L., Goiran, C., Land, L., Jaubert, J., Cuif, J.-P., Allemand, D., 2005. Stable isotopes ($\delta^{13}\text{C}$ and $\delta^{15}\text{N}$)
1735 of organic matrix from coral skeleton. *Proc. Natl. Acad. Sci.* 102, 1525–1530.
1736 <https://doi.org/10.1073/pnas.0408921102>
- 1737 Naumann, M.S., Orejas, C., Wild, C., Ferrier-Pagès, C., 2011. First evidence for zooplankton feeding sustaining
1738 key physiological processes in a scleractinian cold-water coral. *J. Exp. Biol.* 214, 3570–3576.
1739 <https://doi.org/10.1242/jeb.061390>
- 1740 Naumann, M.S., Tolosa, I., Taviani, M., Grover, R., Ferrier-Pagès, C., 2015. Trophic ecology of two cold-water
1741 coral species from the Mediterranean Sea revealed by lipid biomarkers and compound-specific isotope
1742 analyses. *Coral Reefs* 34, 1165–1175. <https://doi.org/10.1007/s00338-015-1325-8>
- 1743 Pride C, Thunell R, Sigman D, Keigwin L, Altabet M, Tappa E. 1999. Nitrogen isotopic variations in the Gulf of
1744 California since the Last Deglaciation: Response to global climate change. *Paleoceanography* 14(3).
1745 doi:10.1029/1999PA900004

Formatted: Font: 11 pt, Font color: Text 1

Formatted: Font color: Text 1

~~Mortensen, P.B., Rapp, H.T., Båmstedt, U., 1998. Oxygen and carbon isotope ratios related to growth line patterns in skeletons of *Lophelia pertusa* (L.) (Anthozoa, Scleractinia): Implications for determination of linear extension rate. *Sarsia* 83, 433–446. <https://doi.org/10.1080/00364827.1998.10413702>~~

Formatted: Font color: Text 1

Formatted: Font: (Default) +Body (Times New Roman), 11 pt, Font color: Text 1

Formatted: Font color: Text 1

Formatted: Font color: Text 1

Formatted: Font color: Text 1

Formatted: Font: 11 pt, Font color: Text 1

Formatted: Font color: Text 1

~~Orejas C, Ferrier-Pagès C, Reynaud S, Tsounis G, Allemand D, Gili JM. 2011. Experimental comparison of skeletal growth rates in the cold water coral *Madrepora oculata* Linnaeus, 1758 and three tropical scleractinian corals. *J Exp Mar Bio Ecol.* 2011;405(1):1–5. doi:<https://doi.org/10.1016/j.jembe.2011.05.008>~~
~~Orejas C, Ferrier-Pagès C, Reynaud S, Gori A and others. 2011. Long-term growth rates of four Mediterranean cold-water coral species maintained in aquaria. *Mar Ecol Prog Ser* 429:57–65. <https://doi.org/10.3354/meps09104>~~
~~Osinga, R., Schutter, M., Griffioen, B. et al. 2011. The Biology and Economics of Coral Growth. *Mar Biotechnol* 13, 658–671 (2011). <https://doi.org/10.1007/s10126-011-9382-7>~~

Formatted: Font color: Text 1

1763 Purser A, Larsson AI, Thomsen L, van Oevelen D. 2010. The influence of flow velocity and food concentration
1764 on *Lophelia pertusa* (Scleractinia) zooplankton capture rates. *J Exp Mar Bio Ecol.* 395(1):55-62.
1765 doi:https://doi.org/10.1016/j.jembe.2010.08.013

1766 Rae, J.W.B. 2018. Boron Isotopes in Foraminifera: Systematics, Biomineralisation, and CO₂ Reconstruction. In:
1767 Marschall, H., Foster, G. (eds) Boron Isotopes. Advances in Isotope Geochemistry. Springer, Cham.
1768 https://doi.org/10.1007/978-3-319-64666-4_5

1769 Rangel, M.S., Erler, D., Tagliafico, A., Cowden, K., Scheffers, S., Christidis, L., 2019. Quantifying the transfer
1770 of prey δ¹⁵N signatures into coral holobiont nitrogen pools. *Mar. Ecol. Prog. Ser.* 610, 33–49.
1771 https://doi.org/10.3354/meps12847

1772 Ren, H., Sigman, D.M., Meckler, A.N., Plessen, B., Robinson, R.S., Rosenthal, Y., Haug, G.H., 2009.
1773 Foraminiferal Isotope Evidence of Reduced Nitrogen Fixation in the Ice Age Atlantic Ocean. *Science*
1774 323, 244–248. https://doi.org/10.1126/science.1165787

1775 Reynaud, S., Martinez, P., Houlbrèque, F., Billy, I., Allemand, D., Ferrier-Pagès, C., 2009. Effect of light and
1776 feeding on the nitrogen isotopic composition of a zooxanthellate coral: role of nitrogen recycling. *Mar.*
1777 *Ecol. Prog. Ser.* 392, 103–110. https://doi.org/10.3354/meps08195

1778 Roberts, J.M., Wheeler, A.J., Freiwald, A., 2006. Reefs of the deep: The biology and geology of cold-water coral
1779 ecosystems. *Science* 312, 543–547. https://doi.org/10.1126/science.1119861

1780 Robinson, R.S., Kienast, M., Albuquerque, A.L., Altabet, M., Contreras, S., Holz, R.D.P., Dubois, N., Francois,
1781 R., Galbraith, E., Hsu, T.-C., Ivanochko, T., Jaccard, S., Kao, S.-J., Kiefer, T., Kienast, S., Lehmann, M.,
1782 Martinez, P., McCarthy, M., Möbius, J., Pedersen, T., Quan, T.M., Ryabenko, E., Schmittner, A.,
1783 Schneider, R., Schneider-Mor, A., Shigemitsu, M., Sinclair, D., Somes, C., Studer, A., Thunell, R., Yang,
1784 J.-Y., 2012. A review of nitrogen isotopic alteration in marine sediments. *Paleoceanography* 27.
1785 https://doi.org/10.1029/2012PA002321

1786 Robinson LF, Adkins JF, Frank N, Gagnon, A.C., Prouty, N.G., Roark, B. van de Fliedert, T. 2014. The
1787 geochemistry of deep-sea coral skeletons: A review of vital effects and applications for
1788 palaeoceanography. *Deep Sea Res Part II Top Stud Oceanogr.* 99:184-198.
1789 doi:https://doi.org/10.1016/j.dsr2.2013.06.005

1790 Robinson RS, Sigman DM. 2008. Nitrogen isotopic evidence for a poleward decrease in surface nitrate within the
1791 ice age Antarctic. *Quat Sci Rev.* 27(9-10). doi:10.1016/j.quascirev.2008.02.005

1792 Robinson, R.S., Smart, S.M., Cybulski, J.D., McMahon, K.W., Marcks, B., Nowakowski, C., 2023. Insights from
1793 fossil-bound nitrogen isotopes in diatoms, foraminifera, and corals. *Annu. Rev. Mar. Sci.* 15, null.
1794 https://doi.org/10.1146/annurev-marine-032122-104001

1795 Ryan, W. B. F., S.M. Carbotte, J. Coplan, S. O'Hara, A. Melkonian, R. Arko, R.A. Weissel, V. Ferrini, A.
1796 Goodwillie, F. Nitsche, J. Bonczkowski, R. Zemsky, 2009. Global Multi-Resolution Topography
1797 (GMRT) synthesis data set. *Geochem. Geophys. Geosyst.*, 10, Q03014. doi:10.1029/2008GC002332

1798 Saino, T., Hattori, A., 1987. Geographical variation of the water column distribution of suspended particulate
1799 organic nitrogen and its ¹⁵N natural abundance in the Pacific and its marginal seas. *Deep Sea Res. A* 34,
1800 807–827. https://doi.org/10.1016/0198-0149(87)90038-0

Formatted: Font: (Default) +Body (Times New Roman),
Font color: Text 1

Formatted: Normal, Indent: Left: 0", Hanging: 0.5", Space
Before: 0 pt, After: 0 pt

Deleted: ¶

Formatted: Font: (Default) +Body (Times New Roman), 11
pt, Font color: Text 1

Formatted: Font: +Body (Times New Roman), Font color:
Text 1

Formatted: Font color: Text 1

Deleted: ¶

Formatted: Hyperlink, Font color: Text 1

Formatted: Font color: Text 1

Field Code Changed

Deleted: Ren,

Deleted: H., Chen, Y.-C., Wang, X.T., Wong, G.T.F., Cohen,
A.L., DeCarlo, T.M., Weigand, M.A., Mii, H.-S., Sigman, D.M.,
2017. 21st-century rise in anthropogenic nitrogen deposition on a
remote coral reef. *Science* 356, 749–752.

Formatted: Font: 11 pt, Font color: Text 1

Formatted: Font: 11 pt, Font color: Text 1

Formatted: Font: Font color: Text 1

Formatted: Font: 11 pt, Font color: Text 1

Formatted: Font color: Text 1

Formatted: Hyperlink, Font color: Text 1

Field Code Changed

Formatted: Font: (Default) +Body (Times New Roman), 11
pt, Font color: Text 1

Formatted: Font color: Text 1

Formatted: Font: (Default) +Body (Times New Roman), 11
pt, Font color: Text 1

Formatted: Font color: Text 1

Formatted: Font: (Default) +Body (Times New Roman), 11
pt, Font color: Text 1

Formatted: Font: (Default) +Body (Times New Roman), 11
pt, Font color: Text 1

Formatted: Font: (Default) +Body (Times New Roman), 11
pt, Font color: Text 1

Formatted: Font color: Text 1

- 1808 Scrimgeour, C.M., Gordon, S.C., Handley, L.L., Woodford, J.A.T., 1995. Trophic levels and anomalous $\delta^{15}\text{N}$ of
 1809 insects on raspberry (*Rubus Idaeus* L.). *Isotopes Environ. Health Stud.* 31, 107–115.
 1810 <https://doi.org/10.1080/10256019508036256>
- 1811 Sebens, K.P., Vandersall, K.S., Savina, L.A., Graham, K.R., 1996. Zooplankton capture by two scleractinian
 1812 corals, *Madracis mirabilis* and *Montastrea cavernosa*, in a field enclosure. *Mar. Biol.* 127, 303–317.
 1813 <https://doi.org/10.1007/BF00942116>
- 1814 Sherwood, O.A., Heikoop, J.M., Scott, D.B., Risk, M.J., Guilderson, T.P., McKinney, R.A., 2005. Stable isotopic
 1815 composition of deep-sea gorgonian corals *Primnoa* spp.: a new archive of surface processes. *Mar. Ecol.*
 1816 *Prog. Ser.* 301, 135–148. <https://doi.org/10.3354/meps301135>
- 1817 Sherwood, O.A., Jamieson, R.E., Edinger, E.N., Wareham, V.E., 2008. Stable C and N isotopic composition of
 1818 cold-water corals from the Newfoundland and Labrador continental slope: Examination of trophic, depth
 1819 and spatial effects. *Deep Sea Res. Part Oceanogr. Res. Pap.* 55, 1392–1402.
 1820 <https://doi.org/10.1016/j.dsr.2008.05.013>
- 1821 Sherwood, O.A., Thresher, R.E., Fallon, S.J., Davies, D.M., Trull, T.W., 2009. Multi-century time-series of ^{15}N
 1822 and ^{14}C in bamboo corals from deep Tasmanian seamounts: evidence for stable oceanographic
 1823 conditions. *Mar. Ecol. Prog. Ser.* 397, 209–218. <https://doi.org/10.3354/meps08166>
- 1824 Sigman, D.M., Altabet, M.A., McCorkle, D.C., Francois, R., Fischer, G., 1999. The $\delta^{15}\text{N}$ of nitrate in the
 1825 Southern Ocean: Consumption of nitrate in surface waters. *Glob. Biogeochem. Cycles* 13, 1149–1166.
 1826 <https://doi.org/10.1029/1999GB900038>
- 1827 Sigman, D., Boyle, E. Glacial/interglacial variations in atmospheric carbon dioxide. 2000. *Nature* 407, 859–869
 1828 (2000). <https://doi.org/10.1038/35038000>
- 1829 Sigman, D.M., Casciotti, K.L., Andreani, M., Barford, C., Galanter, M., Böhlke, J.K., 2001. A Bacterial method
 1830 for the nitrogen isotopic analysis of nitrate in seawater and freshwater. *Anal. Chem.* 73, 4145–4153.
 1831 <https://doi.org/10.1021/ac010088e>
- 1832 Sigman, D.M., Fripiat, F., 2019. *Nitrogen Isotopes in the Ocean*, in: Cochran, J.K., Bokuniewicz, H.J., Yager,
 1833 P.L. (Eds.), *Encyclopedia of Ocean Sciences (Third Edition)*. Academic Press, Oxford, pp. 263–278.
 1834 <https://doi.org/10.1016/B978-0-12-409548-9.11605-7>
- 1835 Soetaert, K., Mohn, C., Rengstorf, A., Grehan, A., van Oevelen, D., 2016. Ecosystem engineering creates a direct
 1836 nutritional link between 600-m deep cold-water coral mounds and surface productivity. *Sci. Rep.* 6,
 1837 35057. <https://doi.org/10.1038/srep35057>
- 1838 Spero, H.J., Andreasen, D.J., Sorgeloos, P., 1993. Carbon and nitrogen isotopic composition of different strains
 1839 of *Artemia* sp. *Int. J. Salt Lake Res.* 2, 133. <https://doi.org/10.1007/BF02905905>
- 1840 Studer, A.S., Sigman, D.M., Martinez-Garcia, A., Thole, L.M., Michel, E., Jaccard, S.L., Lippolds, J.A., Mazaud, A., Wang, X.C.T., Robinson, L.F., Adkins, J.F., Haug, G.H., 2018. Increased nutrient supply to the
 1841 Southern Ocean during the Holocene and its implications for the pre-industrial atmospheric CO₂ rise. *Nat Geosci* 11, 756–761
 1842 <https://doi.org/10.1038/s41561-018-0200-2>
 1843 <https://doi.org/10.1038/s41561-018-0200-2>
- 1844 Tanaka, Y., Miyajima, T., Koike, I., Hayashibara, T., Ogawa, H., 2006. Translocation and conservation of
 1845 organic nitrogen within the coral-zooxanthella symbiotic system of *Acropora pulchra*, as demonstrated

Formatted: Font: 11 pt, Font color: Text 1

Formatted: Font color: Text 1

Deleted: Schutter, M., Crocker, J., Pajmans, A., Janse, M., Ozinga, R., Verreth, J.A.J., Wijffels, R.H. 2010. The effect of different flow regimes on the growth and metabolic rates of the scleractinian coral *Galaxea fascicularis*. *Coral Reefs* 29, 737–748. <https://doi.org/10.1007/s00338-010-0617-2>

Formatted: Font color: Text 1

Formatted: Font: 11 pt, Font color: Text 1

Formatted: Font color: Text 1

Formatted: Font: 11 pt, Font color: Text 1

Formatted: Font color: Text 1

Formatted: Font: 11 pt, Font color: Text 1

Formatted: Font color: Text 1

Formatted: Hyperlink, Font color: Text 1

Field Code Changed

Formatted: Font: (Default) +Body (Times New Roman), 11 pt, Font color: Text 1

Formatted: Indent: Left: 0", Hanging: 0.5"

Deleted: 1

- 1852 by dual isotope-labeling techniques. *J. Exp. Mar. Biol. Ecol.* 336, 110–119.
1853 <https://doi.org/10.1016/j.jembe.2006.04.011>
- 1854 Tanaka, Y., Suzuki, A., Sakai, K., 2018. The stoichiometry of coral-dinoflagellate symbiosis: carbon and nitrogen
1855 cycles are balanced in the recycling and double translocation system. *ISME J.* 12, 860–868.
1856 <https://doi.org/10.1038/s41396-017-0019-3>
- 1857 Teece, M.A., Estes, B., Gelsleichter, E., Lirman, D., 2011. Heterotrophic and autotrophic assimilation of fatty
1858 acids by two scleractinian corals, *Montastraea faveolata* and *Porites astreoides*. *Limnol. Oceanogr.* 56,
1859 1285–1296. <https://doi.org/10.4319/lo.2011.56.4.1285>
- 1860 Thiagarajan N., Subhas A. V., Southon J. R., Eiler J. M. and Adkins J. F. 2014. Abrupt pre-Bolling-Allerod
1861 warming and circulation changes in the deep ocean. *Nature* 511, 75–78.
1862 <https://doi.org/10.1038/nature13472>
- 1863 Thiem, Ø., Ravagnan, E., Fosså, J.H., Berntsen, J., 2006. Food supply mechanisms for cold-water corals along a
1864 continental shelf edge. *J. Mar. Syst.* 60, 207–219. <https://doi.org/10.1016/j.jmarsys.2005.12.004>
- 1865 Thomas, S.M., Crowther, T.W., 2015. Predicting rates of isotopic turnover across the animal kingdom: a
1866 synthesis of existing data. *J. Anim. Ecol.* 84, 861–870. <https://doi.org/10.1111/1365-2656.12326>
- 1867 Treiber, L.A., Fawcett, S.E., Lomas, M.W., Sigman, D.M., 2014. Nitrogen isotopic response of prokaryotic and
1868 eukaryotic phytoplankton to nitrate availability in Sargasso Sea surface waters. *Limnol. Oceanogr.* 59,
1869 972–985. <https://doi.org/10.4319/lo.2014.59.3.0972>
- 1870 Tsounis G, Orejas C, Reynaud S, JM G, Allemand D, Ferrier-Pagès C. 2010. Prey-capture rates in four
1871 Mediterranean cold water corals. *Mar Ecol Prog Ser.* 398:149-155. <https://doi.org/10.3354/meps08312>
- 1872 van Oevelen, P., Duineveld, G., Lavaleye, M., Mienis, Furu, Soetaert, Karlina, H., Carlo H. R., 2009. The cold-
1873 water coral community as hotspot of carbon cycling on continental margins: A food-web analysis from
1874 Rockall Bank (northeast Atlantic). *Limnology and Oceanography*, 54, doi: 10.4319/lo.2009.54.6.1829
- 1875 Vinogradov, M. E. Feeding of the deep-sea zooplankton. 1962. *Rapp. Pv. Reun. Cons. Perm. Int. Exp. Mer.* 153,
1876 114–120.
- 1877 Wang, X.T., Prokopenko, M.G., Sigman, D.M., Adkins, J.F., Robinson, L.F., Ren, H., Oleynik, S., Williams, B.,
1878 Haug, G.H., 2014. Isotopic composition of carbonate-bound organic nitrogen in deep-sea scleractinian
1879 corals: A new window into past biogeochemical change. *Earth Planet. Sci. Lett.* 400, 243–250.
1880 <https://doi.org/10.1016/j.epsl.2014.05.048>
- 1881 Wang, X.T., Sigman, D.M., Prokopenko, M.G., Adkins, J.F., Robinson, L.F., Hines, S.K., Chai, J., Studer, A.S.,
1882 Martínez-García, A., Chen, T., Haug, G.H., 2017. Deep-sea coral evidence for lower Southern Ocean
1883 surface nitrate concentrations during the last ice age. *Proc. Natl. Acad. Sci.* 114, 3352–3357.
1884 <https://doi.org/10.1073/pnas.1615718114>
- 1885 Webb, S., Hedges, R., Simpson, S., 1998. Diet quality influences the $\delta^{13}\text{C}$ and $\delta^{15}\text{N}$ of locusts and their
1886 biochemical components. *J. Exp. Biol.* 201, 2903–2911. <https://doi.org/10.1242/jeb.201.20.2903>
- 1887 Weigand, M.A., Foriel, J., Barnett, B., Oleynik, S., Sigman, D.M., 2016. Updates to instrumentation and
1888 protocols for isotopic analysis of nitrate by the denitrifier method. *Rapid Commun. Mass Spectrom.* 30,
1889 1365–1383. <https://doi.org/10.1002/rcm.7570>

Formatted: Font: 11 pt, Font color: Text 1

Formatted: Font color: Text 1

Formatted: No underline, Font color: Text 1

Formatted: Font: 11 pt, Font color: Text 1

Formatted: No underline, Font color: Text 1

Formatted: Font color: Text 1

Deleted: ¶

Formatted: Font color: Text 1, Strikethrough

Formatted: Font color: Text 1

Formatted: Font: 11 pt, Font color: Text 1

Formatted: Font color: Text 1

1891 Williams, B., and Grotoli, A. G. 2010. Recent shoaling of the nutricline and thermocline in the western tropical
1892 Pacific, *Geophys. Res. Lett.*, 37, L22601, doi:10.1029/2010GL044867.

1893 Zhang, R., X. T. Wang, H. Ren, J. Huang, M. Chen, and D. M. Sigman. 2020. Dissolved Organic Nitrogen
1894 Cycling in the South China Sea From an Isotopic Perspective. *Glob. Biogeochem. Cycles* 34:
1895 e2020GB006551. doi:10.1029/2020GB006551.

1896 Zhou, M., Granger, J., Chang, B.X., 2022. Influence of sample volume on nitrate N and O isotope ratio analyses
1897 with the denitrifier method. *Rapid Commun. Mass Spectrom.* 36, e9224.
1898 <https://doi.org/10.1002/rcm.9224>

Formatted: Font: (Default) +Body (Times New Roman), 11 pt, Font color: Text 1

Formatted: Font color: Text 1

Formatted: Font color: Text 1

Formatted: Font color: Text 1

Deleted: Wishner, K.F., Meise-Munns, C.J., 1984. In situ grazing rates of deep sea benthic boundary layer zooplankton. *Mar. Biol.* 84, 65-74. <https://doi.org/10.1007/BF00394528>

Formatted: Font color: Text 1

Page 1: [1] Formatted Anne M Gothmann 12/6/23 7:59:00 AM

Font: 16 pt, Font color: Text 1

Page 1: [1] Formatted Anne M Gothmann 12/6/23 7:59:00 AM

Font: 16 pt, Font color: Text 1

Page 1: [2] Formatted Anne M Gothmann 12/6/23 7:59:00 AM

Font color: Text 1

Page 1: [2] Formatted Anne M Gothmann 12/6/23 7:59:00 AM

Font color: Text 1

Page 1: [3] Deleted Anne M Gothmann 12/6/23 7:59:00 AM

x

Page 1: [3] Deleted Anne M Gothmann 12/6/23 7:59:00 AM

x

Page 1: [4] Formatted Anne M Gothmann 12/6/23 7:59:00 AM

Font: 16 pt, Font color: Text 1

Page 1: [4] Formatted Anne M Gothmann 12/6/23 7:59:00 AM

Font: 16 pt, Font color: Text 1

Page 1: [5] Formatted Anne M Gothmann 11/14/23 3:33:00 PM

Font: 12 pt

Page 1: [5] Formatted Anne M Gothmann 11/14/23 3:33:00 PM

Font: 12 pt

Page 1: [6] Deleted Masha Prokopenko 11/20/23 1:50:00 PM

x

Page 1: [6] Deleted Masha Prokopenko 11/20/23 1:50:00 PM

x

Page 1: [6] Deleted Masha Prokopenko 11/20/23 1:50:00 PM

x

Page 1: [7] Formatted Anne M Gothmann 11/14/23 3:33:00 PM

Font: 12 pt, Font color: Auto

Page 1: [7] Formatted Anne M Gothmann 11/14/23 3:33:00 PM

Font: 12 pt, Font color: Auto

Page 1: [8] Deleted Anne M Gothmann 12/6/23 8:09:00 AM

x

Page 1: [8] Deleted Anne M Gothmann 12/6/23 8:09:00 AM

x

x

Page 1: [9] Formatted Anne M Gothmann 11/14/23 3:33:00 PM

Font: 12 pt, Font color: Auto

Page 1: [9] Formatted Anne M Gothmann 11/14/23 3:33:00 PM

Font: 12 pt, Font color: Auto

Page 1: [10] Deleted Anne M Gothmann 12/6/23 8:10:00 AM

Page 1: [10] Deleted Anne M Gothmann 12/6/23 8:10:00 AM

Page 1: [11] Formatted Anne M Gothmann 11/14/23 3:33:00 PM

Font: 12 pt

Page 1: [11] Formatted Anne M Gothmann 11/14/23 3:33:00 PM

Font: 12 pt

Page 1: [12] Formatted Anne M Gothmann 11/14/23 3:33:00 PM

Font: 12 pt, Font color: Auto

Page 1: [12] Formatted Anne M Gothmann 11/14/23 3:33:00 PM

Font: 12 pt, Font color: Auto

Page 1: [13] Deleted Anne M Gothmann 12/6/23 8:11:00 AM

Page 1: [13] Deleted Anne M Gothmann 12/6/23 8:11:00 AM

Page 1: [13] Deleted Anne M Gothmann 12/6/23 8:11:00 AM

Page 1: [14] Deleted Masha Prokopenko 11/20/23 2:39:00 PM

Page 13: [15] Deleted Anne M Gothmann 10/17/23 7:54:00 AM

Page 24: [16] Formatted Anne M Gothmann 11/14/23 3:51:00 PM

Indent: First line: 0.25", Space After: 0 pt, Line spacing: 1.5 lines, Don't adjust space between Latin and Asian text, Don't adjust space between Asian text and numbers

Page 24: [17] Deleted Anne M Gothmann 11/14/23 3:44:00 PM

Page 26: [18] Deleted Anne M Gothmann 11/14/23 3:49:00 PM

Page 28: [19] Deleted Anne M Gothmann 10/25/23 10:58:00 AM

Page 28: [19] Deleted Anne M Gothmann 10/25/23 10:58:00 AM

Page 28: [19] Deleted Anne M Gothmann 10/25/23 10:58:00 AM

Page 28: [19] Deleted Anne M Gothmann 10/25/23 10:58:00 AM

Page 28: [19] Deleted Anne M Gothmann 10/25/23 10:58:00 AM

Page 28: [20] Deleted Masha Prokopenko 10/31/23 11:38:00 PM

Page 28: [20] Deleted Masha Prokopenko 10/31/23 11:38:00 PM

Page 28: [21] Formatted Anne M Gothmann 11/14/23 3:33:00 PM

Font color: Text 1

Page 28: [21] Formatted Anne M Gothmann 11/14/23 3:33:00 PM

Font color: Text 1

Page 28: [21] Formatted Anne M Gothmann 11/14/23 3:33:00 PM

Font color: Text 1

Page 28: [21] Formatted Anne M Gothmann 11/14/23 3:33:00 PM

Font color: Text 1

Page 28: [22] Deleted Masha Prokopenko 10/31/23 11:32:00 PM

Page 28: [22] Deleted Masha Prokopenko 10/31/23 11:32:00 PM

Page 28: [23] Formatted Anne M Gothmann 11/14/23 3:33:00 PM

Font: Italic, Font color: Text 1

Page 28: [23] Formatted Anne M Gothmann 11/14/23 3:33:00 PM

Font: Italic, Font color: Text 1

Page 28: [24] Deleted Anne M Gothmann 11/14/23 8:20:00 PM

Page 28: [25] Deleted Masha Prokopenko 11/24/23 6:40:00 AM

▲
Page 28: [25] Deleted Masha Prokopenko 11/24/23 6:40:00 AM

▼
▲
Page 28: [26] Formatted Anne M Gothmann 11/14/23 3:33:00 PM

Font color: Text 1

▲
Page 28: [26] Formatted Anne M Gothmann 11/14/23 3:33:00 PM

Font color: Text 1

▲
Page 28: [27] Deleted Anne M Gothmann 11/14/23 8:18:00 PM

▲
Page 28: [28] Deleted Masha Prokopenko 11/1/23 12:18:00 AM

▲
Page 28: [28] Deleted Masha Prokopenko 11/1/23 12:18:00 AM

▲
Page 28: [28] Deleted Masha Prokopenko 11/1/23 12:18:00 AM

▲
Page 29: [29] Deleted Masha Prokopenko 11/25/23 1:13:00 PM

▲
Page 29: [29] Deleted Masha Prokopenko 11/25/23 1:13:00 PM

▲
Page 29: [30] Deleted Anne M Gothmann 10/16/23 12:21:00 PM

▲
Page 29: [30] Deleted Anne M Gothmann 10/16/23 12:21:00 PM

▲
Page 29: [30] Deleted Anne M Gothmann 10/16/23 12:21:00 PM

▲
Page 29: [31] Deleted Masha Prokopenko 11/1/23 12:23:00 AM

▲
Page 29: [31] Deleted Masha Prokopenko 11/1/23 12:23:00 AM

▲
Page 29: [32] Deleted Masha Prokopenko 11/1/23 12:26:00 AM

x
▲
Page 29: [32] Deleted Masha Prokopenko 11/1/23 12:26:00 AM

x
▲
Page 29: [32] Deleted Masha Prokopenko 11/1/23 12:26:00 AM

x
▲
Page 29: [32] Deleted Masha Prokopenko 11/1/23 12:26:00 AM

x
▲
Page 29: [32] Deleted Masha Prokopenko 11/1/23 12:26:00 AM

x
▲
Page 29: [33] Deleted Anne M Gothmann 10/17/23 8:34:00 AM

x
▲
Page 29: [33] Deleted Anne M Gothmann 10/17/23 8:34:00 AM

x
▲
Page 29: [34] Deleted Anne M Gothmann 10/15/23 9:05:00 AM

x
▲
Page 29: [34] Deleted Anne M Gothmann 10/15/23 9:05:00 AM

x
▲
Page 29: [34] Deleted Anne M Gothmann 10/15/23 9:05:00 AM

x
▲
Page 29: [34] Deleted Anne M Gothmann 10/15/23 9:05:00 AM

x
▲
Page 29: [34] Deleted Anne M Gothmann 10/15/23 9:05:00 AM

x
▲
Page 29: [34] Deleted Anne M Gothmann 10/15/23 9:05:00 AM

x
▲

Page 29: [34] Deleted **Anne M Gothmann** **10/15/23 9:05:00 AM**

Page 29: [34] Deleted **Anne M Gothmann** **10/15/23 9:05:00 AM**

Page 29: [35] Formatted **Anne M Gothmann** **11/14/23 3:33:00 PM**

Font color: Text 1

Page 29: [35] Formatted **Anne M Gothmann** **11/14/23 3:33:00 PM**

Font color: Text 1

Page 29: [36] Formatted **Anne M Gothmann** **11/14/23 3:33:00 PM**

Font color: Text 1

Page 29: [36] Formatted **Anne M Gothmann** **11/14/23 3:33:00 PM**

Font color: Text 1

Page 29: [37] Deleted **Masha Prokopenko** **11/1/23 12:29:00 AM**

Page 33: [38] Formatted **Anne M Gothmann** **12/20/23 7:44:00 AM**

Font: (Default) Times New Roman, No underline, Font color: Text 1

Page 33: [39] Formatted **Anne M Gothmann** **12/20/23 7:44:00 AM**

Font: +Body (Times New Roman), 11 pt, No underline, Font color: Text 1

Page 33: [40] Formatted **Anne M Gothmann** **12/20/23 7:44:00 AM**

Font: (Default) +Headings (Times New Roman), 11 pt, No underline, Font color: Text 1

Page 33: [41] Formatted **Anne M Gothmann** **12/20/23 7:44:00 AM**

Font: (Default) +Headings (Times New Roman), Font color: Text 1